PNNL-29145

Pacific Northwest
NATIONAL LABORATORY

Relaying for Distribution and Microgrids

Evolving from Radial to Bidirectional Power Flow

September 2019

TE McDermott
R Fan
P Thekkumparambath Mana
B Vyakaranam
TM Smith
JC Hambrick
Z Li
AK Barnes

U.S. DEPARTMENT OF ENERGY

Prepared for the U.S. Department of Energy
under Contract DE-AC05-76RL01830

DISCLAIMER

PACIFIC NORTHWEST NATIONAL LABORATORY
operated by
BATTELLE
for the
UNITED STATES DEPARTMENT OF ENERGY
under Contract DE-AC05-76RL01830

Printed in the United States of America

Available to DOE and DOE contractors from the
Office of Scientific and Technical Information,
P.O. Box 62, Oak Ridge, TN 37831-0062;
ph: (865) 576-8401
fax: (865) 576-5728
email: reports@adonis.osti.gov

Available to the public from the National Technical Information Service
5301 Shawnee Rd., Alexandria, VA 22312
ph: (800) 553-NTIS (6847)
email: orders@ntis.gov <http://www.ntis.gov/about/form.aspx>
Online ordering: http://www.ntis.gov

PNNL-29145

Relaying for Distribution and Microgrids

Evolving from Radial to Bidirectional Power Flow

September 2019

TE McDermott
R Fan
P Thekkumparambath Mana
B Vyakaranam
TM Smith[1]
JC Hambrick[1]
Z Li[1]
AK Barnes[2]

Prepared for
the U.S. Department of Energy
under Contract DE-AC05-76RL01830

[1] Oak Ridge National Laboratory
[2] Los Alamos National Laboratory

Abstract

As distributed energy resources (DERs) achieve higher penetration levels in distribution systems, the normal flow of power (and fault current) is no longer unidirectional, from substation source to load (or fault). The increased importance of DERs has also led to revisions in the DER interconnection standards, particularly voltage regulation and ride-through, with publication of a new IEEE Standard 1547-2018. These changes have complicated normal distribution system operation, and they will also complicate distribution system protection. The U.S. Department of Energy undertook a review of the protection state of the art for this new environment in order to identify gaps and propose near-term solutions.

Executive Summary

As distributed energy resources (DERs) achieve higher penetration levels in distribution systems, the normal flow of power (and fault current) is no longer unidirectional, from substation source to load (or fault). Bidirectional fault currents can defeat the traditional distribution system protection schemes, which assume that fault current steadily decreases with fault distance from the substation. The increased importance of DERs has also led to revisions in the DER interconnection standards, particularly voltage regulation and ride-through, with approval of a new version of IEEE Standard 1547 in early 2018. These changes have complicated normal distribution system operation, and they will also complicate distribution system protection. This report summarizes a review of distribution system state of the art for this new environment, identifies gaps, and proposes near-term solutions.

A set of metrics was developed for evaluating new protection schemes, shown below. The first three metrics are considered must-pass, while the others may be used for ranking candidates.

Table E.1. Metrics for Evaluating Protection Schemes

Metric	Category	Criterion or Quantity
1	Dependability	Must detect all faults within the protected zone; **failures are disqualifying**.
2	Security	Must not trip for any fault outside the protected zone; **failures are disqualifying**.
3	Selectivity	Must trip the minimum number of devices to isolate the fault, after any reclosing activity has completed. Primary protection must trip before backup protection. **Failures are disqualifying**.
4	Sensitivity	Maximum ground fault resistance before the scheme fails to operate for a ground fault. This can be presented in the form of a graph of resistance vs. fault location.
5	Speed	Time between fault inception and a relay command to trip. This can be presented in the form of a graph of time vs. fault location for different types of fault.
6	Cost (Equipment)	Expected purchase, design, and installation costs for all relays and sensors, per feeder, including both utility-owned and DER relays for a high-penetration case.
7	Cost (Communication)	Expected purchase, design, and installation costs for new communications infrastructure, per feeder, to support the new scheme. Significant communication costs are disqualifying for now.
8	Cost (Labor)	Expected training and engineering costs for a new scheme, per utility, consulting, or DER organization.
9	Flexibility	The highest DER penetration level, defined as DER Capacity / Peak Load, for which no disqualifying failures occur.
10	Maturity (TRL)	The Technology Readiness Level of commercial products that could implement the new scheme.
11	Maturity (Market)	The number of vendors that currently supply products that could implement the scheme.

Based on evaluations that included computer modeling and simulation, three schemes were identified for development and demonstration on radial systems. Work on these will begin in October 2019. They are

1. Focused directional relays, which are widely available and should work for conventional DERs. They may not work for inverter-based DERs.
2. Incremental distance relays may be agnostic to the amount and type of DER. However, they will not generate a persistent trip signal and will always require a completely different non-distance method of backup protection.

3. Traveling-wave relays would also be agnostic to the amount and type of DER. They are more demanding of sensors and timing sources than other schemes. They may be difficult to apply on radial feeders with many taps, or on underground systems. They also do not generate persistent trip signals and will always require a completely different non-wave method of backup protection.

During the evaluation, deficiencies, and uncertainties in the modeling of inverter-based DERs were noted. The magnitude and angle of inverter-supplied fault current are both important, and both differ significantly from conventional DERs. These uncertainties will have to be addressed before utility engineers can perform protection studies with confidence. The U.S. Department of Energy involvement could help spark the necessary collaborations between relay vendors, inverter vendors, and commercial software tool vendors.

An early version of this report was presented at the U.S. Department of Energy headquarters on April 5, 2018. Elements of it were presented to industry peer reviewers at a meeting in Oak Ridge, Tennessee, on July 19–20, 2018. A conference paper on the results was presented at the Western Protective Relay Conference in Spokane, Washington, on October 18, 2018. This report will help inform the development of a protection system research roadmap by the U.S. Department of Energy, which should address microgrids, secondary networks, and longer-term research needs in more detail.

Acknowledgments

The authors thank their project client at the U.S. Department of Energy: David Howard, Office of Electricity. We are also grateful to David R. Smith, PE, for helpful discussions about secondary network operation and protection.

Acronyms and Abbreviations

ACSR	aluminum cable, steel reinforced
AMI	advanced metering infrastructure
ATP	Alternative Transients Program
CN	concentric neutral (cable)
COMTRADE	Common format for Transient Data Exchange
CT	current transformer
DER	distributed energy resource
DOE	U.S. Department of Energy
DST	discrete S-transform
DTT	direct transfer trip
NWP	network protector
NWPR	network protector relay
PCC	point of common coupling
PLL	phase-locked loop
PR	proportional-resonant (controller)
PV	photovoltaic
R1	positive-sequence resistance
RMS	root mean square
SLGF	single line-to-ground fault
SWB	switchboard
UV	undervoltage trip function
VT	voltage transformer

Variables

a	a constant between 0 and 1
b	a constant between 0 and 1
f	frequency
i_{12}	current from bus 1 to bus 2
i_{21}	current from bus 2 to bus 1
I_A	phase A current
$I_{a\Delta}$	phase A difference in current, between the present time and one cycle earlier
j	time index in a discrete Fourier transform
k	a constant less than $\sqrt{a^2 + b^2}$
m	shift index
n	frequency index in a discrete Fourier transform
N	number of points in a discrete Fourier transform
R_{lg}	line-to-ground fault resistance
v	traveling-wave velocity
V	voltage
v_0	zero-sequence wave velocity
v_1	positive-sequence wave velocity
V_a	phase A voltage
$V_{a\Delta}$	phase A difference in voltage, between the present time and one cycle earlier
V_{op}	operating voltage
V_{ref}	reference voltage
X_1	positive-sequence reactance
X_{lg}	line-to-ground fault reactance
Z_0	zero-sequence characteristic impedance
Z_1	positive-sequence characteristic impedance
Z_c	characteristic impedance
Z_{HSD}	high-side detection zone impedance
τ	wave travel time

Contents

Figures

Tables

1.0 Introduction

As distributed energy resources (DERs) achieve higher penetration levels in distribution systems, the normal flow of power (and fault current) is no longer unidirectional, from substation source to load (or fault). Bidirectional fault currents can defeat the traditional distribution system protection schemes, which assume that fault current steadily decreases with fault distance from the substation. The increased importance of DERs has also led to revisions in the DER interconnection standards, particularly voltage regulation and ride-through, which were approved in early 2018 (IEEE 2018). These changes have complicated normal distribution system operation, and they will also complicate distribution system protection. This report summarizes a review of distribution system state of the art for this new environment, identifies gaps, and proposes near-term solutions.

1.1 Scope

The scope of this report covers three task goals:

1. identify various state-of-the-art solutions for protective relaying in a bidirectional power flow environment at the distribution and microgrid levels.
2. identify which solutions will be best applied on distribution (interconnected and radial) and microgrid systems, and rank them accordingly based on protection metrics, effectiveness, cost, complexity, types of information required, types of supporting infrastructure required, and experience level of the protection engineers who will implement them.
3. determine gaps related to bidirectional flow that are not addressed by the state-of-the-art solutions.

Technically, the analysis is partitioned into three different types of distribution system:

1. radial distribution, in which power and fault current have flowed only from substation to loads. If significant generation existed on such a feeder, the feeder was no longer considered radial and was analyzed as a special case. Most of the United States is served by radial distribution, and has only one significant source at the substation.
2. secondary networks, in which radial medium-voltage feeders supply a low-voltage network for greater reliability. Many U.S. urban areas are served this way.
3. microgrids, which are medium-voltage or low-voltage networks. Other than for facility standby power, microgrids are relatively new to the United States.

The focus will be on adaptive settings and other schemes that can work under a variety of bidirectionality conditions. Adaptive relaying includes automatic switching of device settings and functions to match operating conditions, e.g., thunderstorm vs. clear day, or grid connected vs. islanded. Other schemes include those previously applied on transmission only, such as traveling-wave or incremental distance relays. As shown later, a flexible mixture of relay functions may be required. Technologies that focus on control, as opposed to protective relaying, are outside the scope of this effort.

1.2 Summary of DER Interconnection Requirements in IEEE 1547

IEEE 1547-2018 defines two categories of DER for voltage regulation and reactive power control:

1. Category A – minimum performance
2. Category B – for high-penetration scenarios

and three categories for response to disturbances:

1. Category I – essential needs of the bulk power system
2. Category II – ride-through compatible
3. Category III – for high-penetration scenarios.

As in earlier versions, the new 2018 standard states requirements that DER cease to energize the utility power system and trip during faults. “Cease to energize” means no active power delivery, but in the 2018 version, limited reactive power exchange is allowed. This reactive power limit is 3% or 10% of nameplate, depending on size, and must only come from passive devices that serve the DER. During ride-through scenarios, the DER may provide dynamic reactive power for voltage support. As in earlier versions, the DER must coordinate with utility ground fault protection and automatic reclosing practices, but “cease to energize” (i.e., no trip) meets the coordination requirement for reclosing. For unintended islands, the default time to detect and cease to energize is still 2.0 s, but the new 2018 standard allows adjustability up to 5.0 s. These are all functional requirements, and not explicitly linked to undervoltage (UV) trip settings.

Table 1.1 summarizes the UV trip settings in different versions of IEEE 1547 (Note: UV numbers were not used before 2018, but Table 1.1 adopts the 2018 numbering scheme for earlier versions in order to facilitate comparisons). The UV2 function has often been used as de facto fault detection, or backup fault detection, especially for inverter-based DERs. For Category III DER, in high-penetration scenarios, the default UV2 trip time has increased from 0.16 to 2.00 s and may be adjusted up to 21.0 s. This impairs the de facto use of UV2 for fault detection. Other complicating factors may include the increase in islanding detection time, and the allowance for dynamic reactive power during voltage disturbances.

Table 1.1. Undervoltage Trip Requirements in IEEE 1547

	Default		Maximum	
Description	V (p.u.)	Time (s)	V (p.u.)	Time (s)
1547-2003 UV1	0.88	2.00	n/a	n/a
1547-2003 UV2	0.50	0.16	n/a	n/a
1547-2014a UV1	0.88	2.00	n/a	21.0
1547-2014a UV2	0.60	1.00	n/a	11.0
1547-2014a UV3	0.45	0.16	n/a	1.0
1547-2018 Cat I UV1	0.70	2.00	0.88	21.0
1547-2018 Cat I UV2	0.45	0.16	0.50	2.0
1547-2018 Cat II UV1	0.70	10.00	0.88	21.0
1547-2018 Cat II UV2	0.45	0.16	0.50	2.0
1547-2018 Cat III UV1	0.88	21.0	0.88	50.0
1547-2018 Cat III UV2	0.50	2.00	0.50	21.0

1.3 Characteristics of DER for Protection

Many of the concerns with DER protection depend on the magnitude and angle of fault current from the DER. There are important differences between the types of DERs, with respect to fault current magnitude and angle:

- Rotating-machine DER includes backup generators combined heat and power, landfill gas, small hydroelectric, and older wind turbine generators of Types 1–3. A rotating machine is represented by a voltage source behind impedance, or a Thevenin equivalent circuit (Figure 1.1, left), and it provides 5–6 times the rated current to a fault on its terminals. During a fault, the phase relationship between the terminal voltage and the current can change suddenly, because the Thevenin source angle does not change very much, due to inertia and the relatively slow machine excitation controls. On a radial distribution feeder, such DERs behave similarly to the substation source, but is not as strong.
- Inverter-based DERs include primarily solar photovoltaic (PV) power and batteries, but also newer wind turbine generators of Type 4 and fuel cells. These are represented by a voltage-controlled current source in parallel with an impedance, or Norton equivalent (Figure 1.1, right). Fast-acting inverter controls limit the fault contribution to no more than twice the rated current, and usually no more than 1.1 times the rated current. The inverter controls may also act quickly to hold a constant phase angle between current and voltage, so the source angle can change quickly. On a radial distribution feeder, such DERs provide little fault current on their own, although certain types of interconnection transformers may contribute significant ground fault current (Arritt and Dugan 2008, 2015).

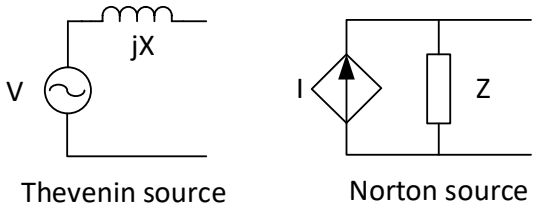

Figure 1.1. Thevenin Source for Conventional DER and Norton Source for Inverter DER

Inverter-based DER may self-protect during a close-in fault, primarily when transient overcurrents occur in the semiconductor switches, or when transient overvoltages occur on the DC link. When the DER ceases to energize the grid for self-protection, it has effectively also tripped for grid fault protection. Otherwise, the inverter-based DER probably does not provide enough fault current for conventional overcurrent relays to trip. For such cases, the undervoltage trip function mandated in IEEE 1547 has provided some de facto fault protection. In its original version,

- When any monitored voltage falls below 50% for 0.16 s, the DER must cease to energize the grid. Depending on the type of connection, (delta, wye, or single phase), both phase-to-neutral and phase-to-phase voltages must be monitored on all phases.
- Each phase-to-phase voltage is monitored for the trip decision, unless the DER is single phase or coupled through a wye-wye transformer, in which case each phase-to-neutral voltage is monitored.
- When any monitored voltage falls below 88% for 2.00 s, the DER must cease to energize the grid. This set point is less useful than the 50% trip for fault detection.

Although the standard does not state the purpose of an undervoltage trip, this function has provided de facto islanding and fault detection, at least in a backup role. However, it does not distinguish between faults on the connected feeder, adjacent feeders, or the transmission system. IEEE 1547-2018 has been

published, and it has changed the undervoltage trip function so that it provides voltage ride-through for faults outside of the connected feeder.

DER interconnections have several protective functions required, depending on the size of DER, for example (National Grid 2018). The minimal set of devices and functions for any size of DER includes

- Device[1] 81, underfrequency and overfrequency trip, mandated in IEEE 1547.
- Device 59, overvoltage trip, mandated in IEEE 1547.
- Device 27, undervoltage trip, mandated in IEEE 1547; device 27 also contributes to grid fault detection.

There are other functions that apply to larger DERs, or that may be required from the utility. Those that may help with grid fault detection include

- Device 59G, a 3V0[2] overvoltage trip that uses voltage inputs from the high side of a delta-wye DER interconnection transformer. The 3V0 value helps the DER detect ground faults on the primary feeder. Otherwise, these are not visible on the low (wye) side.
- Devices 51 and 51N, overcurrent, are primarily intended to protect the rotating machine, but may also trip the machine during grid faults.
- Devices 46 and 47, negative-sequence current and voltage trip, are primarily intended to protect the rotating machine from overheating during unbalanced conditions. These are set sensitive and may trip the machine during grid faults that produce negative-sequence current (i.e., line-to-ground, line-to-line, line-to-line-to-ground).

Many other functions are defined for the larger DER, but they are unlikely to help with grid fault protection. These include Devices 32 (reverse power), 25 (synchronization check before closing), 87 (differential within the machine), and 40 (loss of field). However, feeder protection studies ought to include the DER protection functions that could help with grid fault detection.

1.4 Existing Practices – Radial Distribution

Figure 1.2 shows a simple radial distribution system serving one load, until a fault occurs near the middle of the line. When the fault occurs, the voltage at both the point of the fault and downstream approaches zero, so that load current no longer flows to the load. However, the total fault current through the breaker increases, based on the low line impedance and the higher voltage drop between the breaker and the fault location. Protective relays at the breaker location determine that a downstream fault has occurred by the increase in current magnitude. The fault current should be at least 2× the load current, and is usually significantly higher than that. Figure 1.2 also illustrates a change in voltage, Δv, at the breaker/relay location caused by the fault. This Δv forms the basis for distance relaying on transmission lines, and it shows why the undervoltage trip mandated in IEEE 1547 has provided a form of fault detection. As the fault location moves closer to the breaker, both the fault current and Δv will increase. The fault current can only flow from left to right in Figure 1.2, but we have ignored the possible effects of nonzero fault resistance and different fault types (e.g., line-to-ground, line-to-line, open conductor).

[1] Device numbers are ANSI standard device numbers. Definitions can be found in IEEE C37.2-2008, IEEE Standard Electrical Power System Device Function Numbers, Acronyms, and Contact Designations.
DOI: 10.1109/IEEESTD.2008.4639522.

[2] 3V0 is three times the zero-phase-sequence component of a three phase-to-ground voltage.

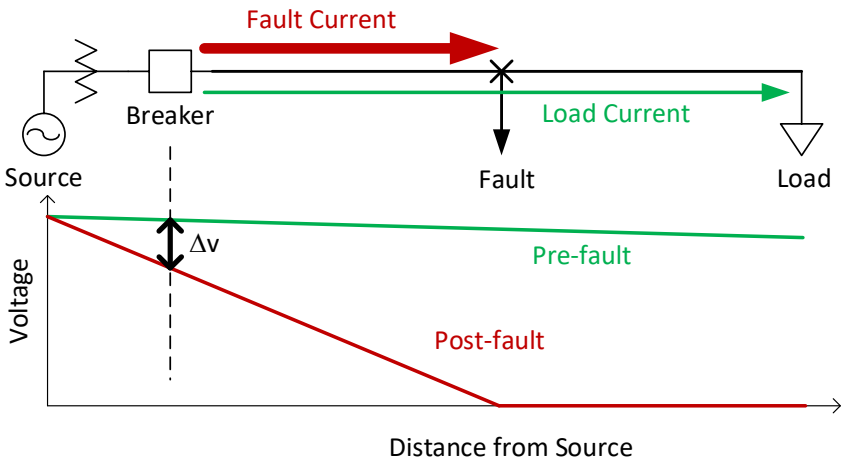

Figure 1.2. Effect of Fault on Current and Voltage on a Radial Feeder

Figure 1.3 shows example time-current curves for a recloser (upper right photo) and expulsion fuse (lower right photo). Fuses are cost-effective fault protection but must be replaced after they "operate." Line reclosers cost more than fuses (about $50 K installed), but they restore service automatically, with sensing, relaying and current interruption provided in a single package. Reclosers are usually mounted on a pole, but they might also be found inside smaller substations, taking the place of feeder breakers. Many utilities have employed a practice known as fuse saving, in which the upstream breaker trips faster than the fuse melts, and then attempt a reclose. If the fault has cleared itself, reclosing succeeds, and every customer on that feeder will have experienced a light-blinking momentary outage. If the fault has not cleared (e.g., vehicle strike on a pole), reclosing fails and the fuse melts. Every customer on that feeder will have experienced a momentary outage, but customers downstream of the fuse will experience a sustained outage of an hour or more. Reclosing succeeds at least half of the time, which usually improves the utility's reliability metrics (IEEE 2012).

The two **red** curves in Figure 1.3 represent the fuse's minimum melt and total clearing characteristics. In a fuse-saving scenario, given the calculated magnitude of fault current, the upstream recloser must open faster than the time read from the minimum melt curve, with some margin that depends on utility practice. Otherwise, the fuse might be damaged even though it did not fully melt. The **blue** fast recloser curve accomplishes this for currents up to about 800 A. If the fault is still present after a fast clearing and automatic reclose, then the recloser needs to wait longer than the time read from the total clearing curve, with some margin that depends on utility practice. Otherwise, the fuse may not melt completely. The **green** slow recloser curve accomplishes this for currents higher than about 120 A. The two devices are said to coordinate for fault currents between 120 and 800 A. The recloser could be set to trip once on the fast curve, and then up to three more times on the slow curve. This process of setting the devices to work properly for different fault types and locations can be automated in computer software, as these procedures were previously laid out in guidebooks.

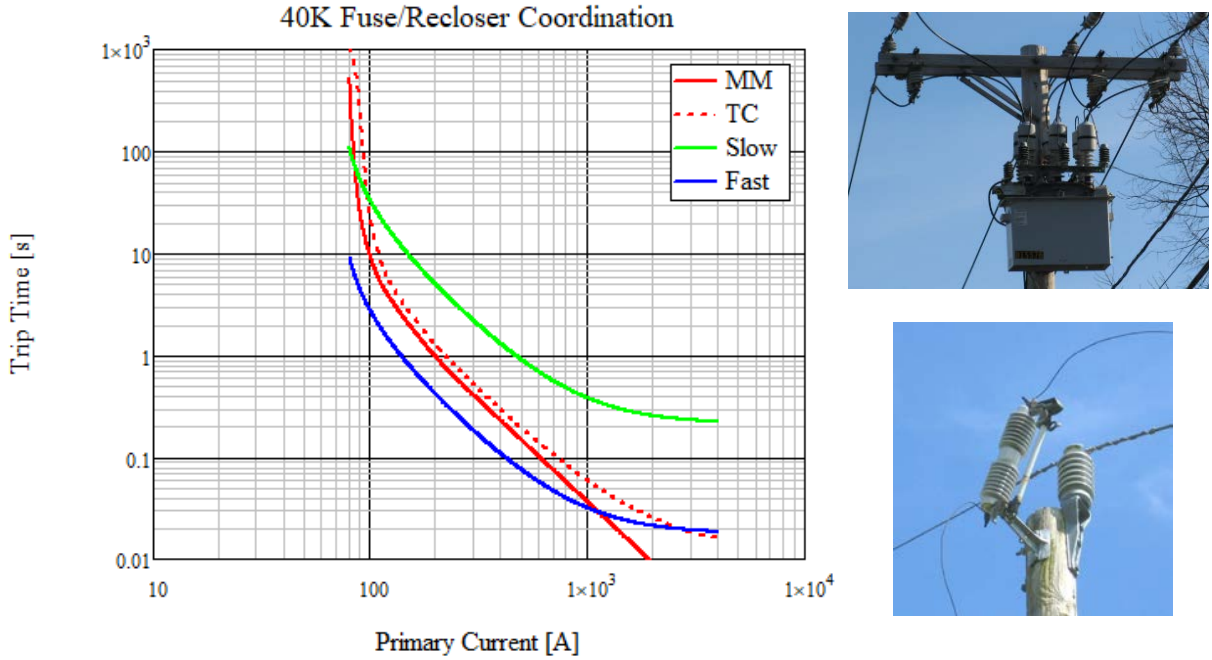

Figure 1.3. Time-Current Curve Coordination for a Recloser and Fuse

Figure 1.4 shows a substation serving two radial feeders, with a DER on the topmost feeder. The topmost feeder also has a fused lateral line tap and a line recloser. If a fault occurs downstream of the recloser, say at the **red X**, both the breaker and recloser see the same magnitude of fault current. The recloser needs to be set so that it trips before the feeder breaker, for that level of fault current. If the recloser fails to trip and clear the fault for some reason, then the feeder breaker must trip as backup protection. Backup tripping harms the reliability metrics because loads between the feeder breaker and the recloser lose service unnecessarily.

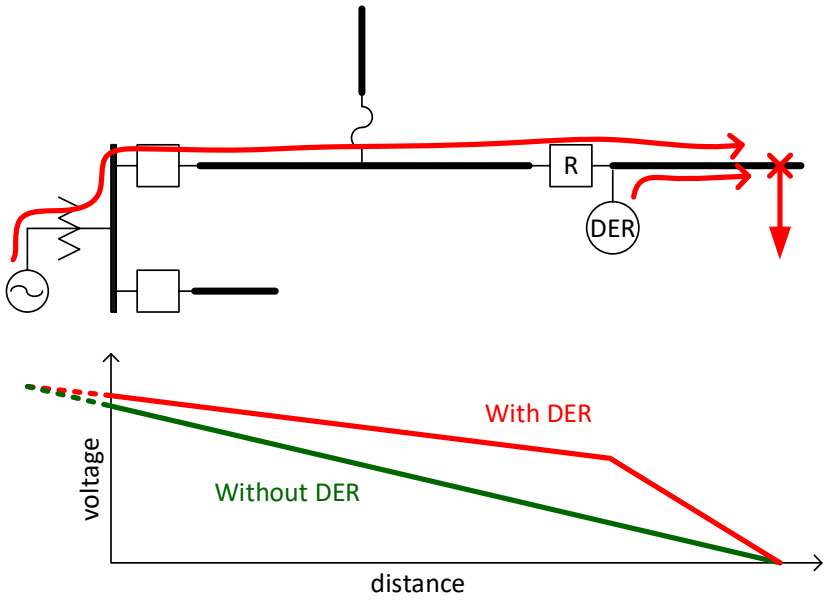

Figure 1.4. Effect of DER on Radial Feeder Faults: Desensitization

When DER is located between the substation and the fault, certain types of DER will help boost the voltage at locations between the substation and the DER. Compare the voltage profiles in Figure 1.2 and Figure 1.4. The effect is to reduce the current seen by the feeder breaker, such that if the line recloser fails to trip for some reason, the feeder breaker will not see enough fault current to trip in its backup role. This issue disappears after the DER trips, as mandated by IEEE 1547. The issue is also less important for inverter-based DER, but it can arise again with ground fault coordination when the interconnection transformer provides an effective ground source (Arritt and Dugan 2008).

Figure 1.5 shows that with DER on the feeder, faults downstream of the lateral fuses experience more fault current than without DER. In some cases, the fuse could melt before the feeder breaker has a chance to trip. With reference to Figure 1.3, this means the blue and red lines cross. The issue is less important with inverter-based DER, which supplies less fault current than other types. Some utilities have already abandoned fuse saving to improve certain voltage quality metrics (i.e., trading large numbers of momentary outages for a smaller number of sustained outages).

Figure 1.6 shows that DER may contribute fault current into faults on another feeder served from the same substation. IEEE 1547 does not mandate that the DER trip for adjacent feeder faults, and in fact, this is a scenario where ride-through is desirable. However, if the DER is large enough and close enough to the substation, it could provide enough reverse fault current through its own feeder breaker to trip that feeder breaker. The fix has been fairly simple: to replace any nondirectional overcurrent relays with directional overcurrent relays on feeder breakers. A directional overcurrent relay trips only when the fault is on the correct side of the relay. To determine this direction, the relay needs a voltage input in addition to the current input. Sympathetic tripping is less likely for inverter-based DER.

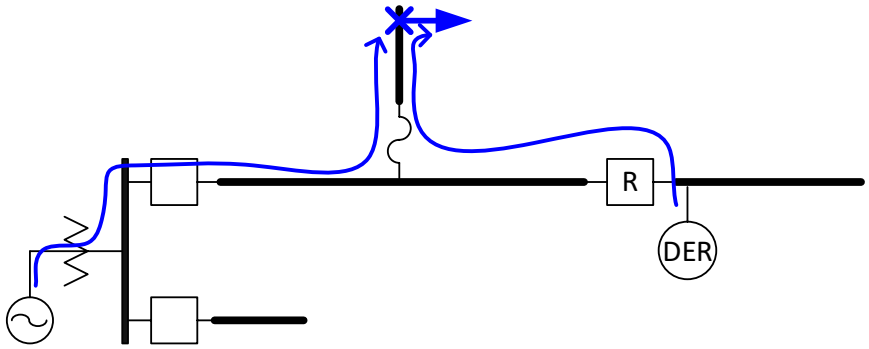

Figure 1.5. Effect of DER on Radial Feeder Faults: Fuse Saving Defeated

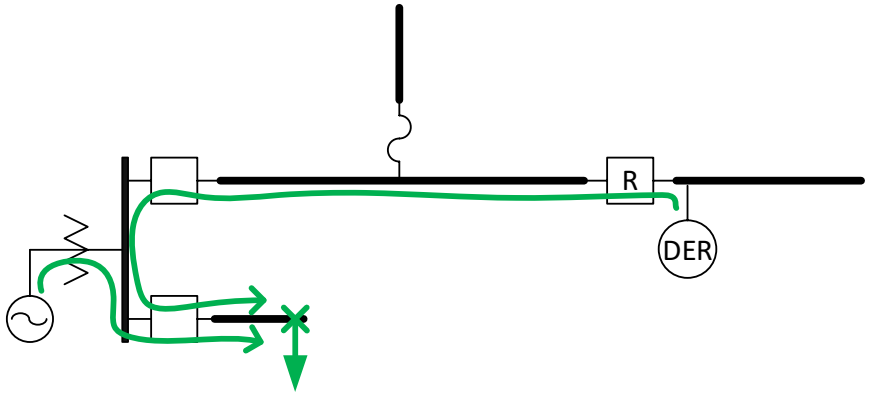

Figure 1.6. Effect of DER on Radial Feeder Faults: Sympathetic Tripping

Figure 1.4 through Figure 1.6 illustrated three scenarios in which DER might compromise protective device coordination on radial distribution. These have been successfully addressed at existing DER penetration levels, i.e., with one or two large DERs on the circuit, or with a moderate level of rooftop solar PV.

Pilot-wire and distance relays have been used for decades on transmission lines, and both schemes include the notion of a "transfer trip," in which relays at one end of a line initiate tripping at the other end. On radial distribution, transfer trips have also been used, but not in the context of a point-to-point line segment. Radial distribution feeders have many branches and loads, and lately, DER installations, that do not usually appear directly connected to transmission lines.

Figure 1.7 shows a direct transfer trip (DTT) scheme that has been used to prevent unintentional islands on a distribution system. It would also provide fault protection. When there is a mixture of DER types on a feeder, the single-device tests mandated in UL1741 (or IEEE 1547.1) do not guarantee that unintentional islands will be detected. The standard tests can show that a single islanded DER unit will trip, even if load and generation perfectly match within the island. Those detection schemes may be defeated if there are different types of DER within the island, especially if those DERs include any rotating machines. DTT has been a method of guaranteeing that multi-DER islands will be de-energized within 2 s. However, DTT is expensive enough to present a barrier to DER integration, especially in remote areas.

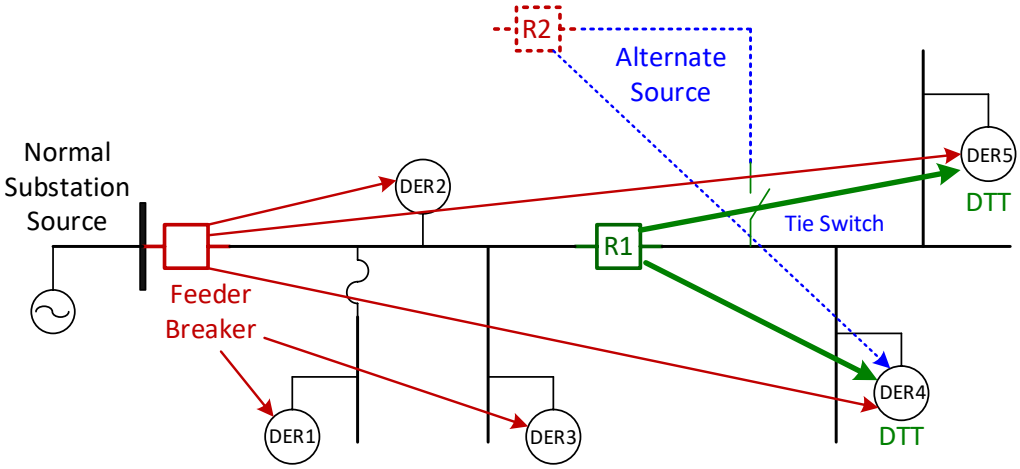

Figure 1.7. DTT on Radial Distribution

In Figure 1.7, closed devices are shown in **red** and open devices are shown in **green**. Because recloser R1 has tripped, it creates an unintended island with DER4 and DER5. Both DERs should cease to energize this island, but in high-penetration scenarios, this may not occur fast enough. DTT would send a high-speed trip signal (shown in **green**) from R1 to both DER4 and DER5. If instead the feeder breaker trips, it creates an unintended island that includes all five DERs. The feeder breaker DTT sends a trip signal (shown in **red**) to each of those five DER units. If a fault caused the feeder breaker or line recloser to trip, then of course each DER should also trip on its own for the fault. However, a breaker or line recloser may open under non-fault conditions, and the DTT scheme works for those conditions. High-speed and high-reliability communications are required to implement DTT.

Some feeders have more than one recloser and more than five DER units, which would increase the cost and complexity. Furthermore, feeder segments are often switched to alternate sources during maintenance or storm restoration. For example, in Figure 1.7, the recloser R1 could open and the normally open tie switch could close, so that DER4 and DER5 would now be connected through the alternate source,

recloser R2. This recloser would be on another feeder, served from the same or a different substation. However, if this condition was not studied or incorporated into the DTT scheme, the utility may require that DER4 and DER5 not operate while served from the alternate source. If not, DTT would have to trip DER4 and DER5 from R2 and any recloser or breakers behind it, as well as from R1 and its feeder breaker. Figure 1.7 shows the DTT signals from R2 in **blue**.

DTT has been applied, in limited circumstances, to relatively large DER. Even so, DTT has been controversial with DER project developers because of the added interconnection expense, which can range from $60 K for hardwiring to an existing DTT, to $600 K for a new DTT (PG&E 2018). Once the larger DERs have tripped, smaller DERs (e.g., rooftop solar) are less likely to maintain an island because load and generation are less likely to match. However, this may not hold true as the penetration of rooftop solar increases.

A type of permissive transfer trip has been proposed to replace DTT (Wang et al. 2009), and it has been successfully demonstrated. A small waveform perturbation is injected onto the system voltage at the substation bus, and each DER must detect this perturbation and interpret it as a signal (the **heartbeat signal**) in order to continue operating. If either R1 or its feeder breaker opens, the heartbeat signal will be interrupted for any downstream DERs, and they would trip. Figure 1.8 shows this for the case of R1 being open, leading to loss of the signal at DER4 and DER5. This tripping could occur fast enough to serve as backup islanding detection, which would include detecting islands created by faults that the DER failed to detect and clear. For example, if all the DERs are inverter based, there may be enough utility-supplied fault current for R1 and/or the feeder breaker to trip. Even if the DERs do not trip on overcurrent, undervoltage, or self-protection, they will eventually trip on loss of the heartbeat signal. Compared to DTT, this scheme accommodates more DER units or additional reclosers without major overhaul.

The DER1–DER5 units could also be allowed to operate from an **alternate heartbeat** signal without implementing DTT. The alternate heartbeat may come from a different substation and have a different signature, so each DER would have to recognize it properly. Figure 1.9 shows DER4 and DER5 continuing to operate with an alternate heartbeat signal coming through R2, after R1 is opened and the tie switch is closed. If the DER units had already tripped when R1 opened, this alternate heartbeat signal would allow them to reconnect automatically.

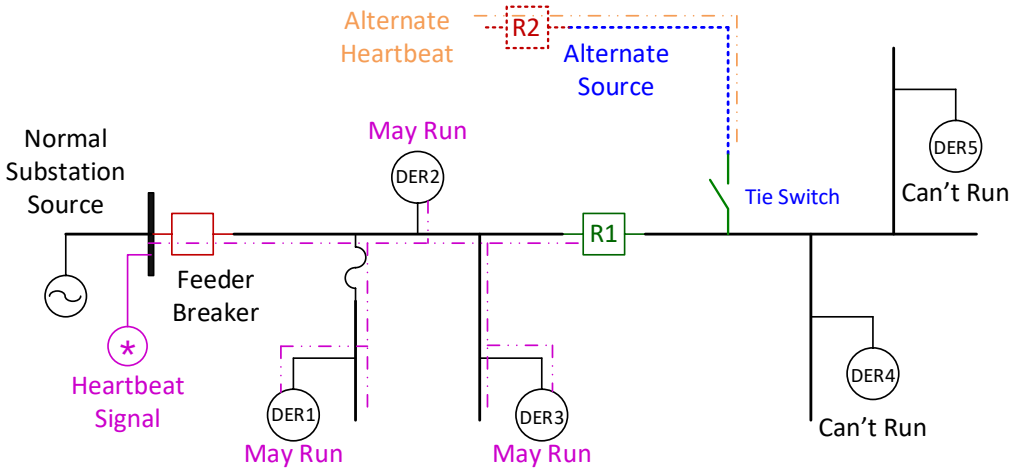

Figure 1.8. Permissive Transfer Trip on Radial Distribution

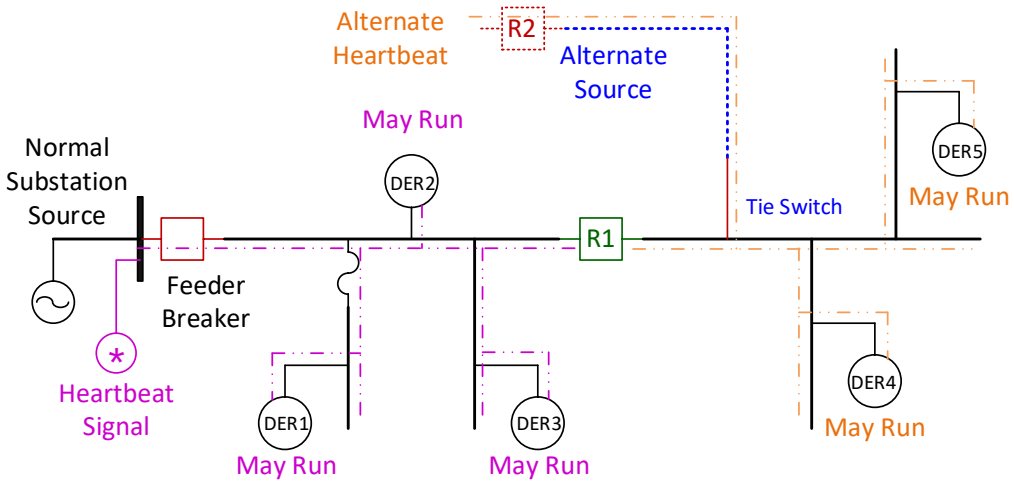

Figure 1.9. Permissive Transfer Trip with an Alternate Source

1.5 Existing Practices – Reclosing and Autoloops

Because at least half of distribution system faults will clear themselves after de-energization, utilities generally attempt one to three automatic reclosings after a breaker or line recloser trips. Figure 1.7 through Figure 1.9 showed a feeder partitioned in two segments, with automatic reclosing on both segments and a manually switched alternate feed. Additional segments and automatic switches would create an "autoloop" system, shown in Figure 1.10. If a fault occurs at the location shown, recloser R3 would open to clear it, leading to loss of voltage at R4, and on the R4 side of R5; see Figure 1.11. After an automatic sequence of time-delayed reclosing attempts, the system in settles into a new operating state, with R3 and R4 open, and R5 closed. Only customers connected between R3 and R4 are out of service, which is the minimum number possible. The new system configuration in Figure 1.12 is still radial.

The autoloop system can be further enhanced with S&C IntelliRupters at the segment boundaries (McCarthy et al. 2008, McCarthy and Staszesky 2008). Autoloops can be implemented with S&C IntelliTeam switches, which can only switch load current. Replacing those switches with IntelliRupters adds the following functions:

- a fault-interrupting recloser with phase and ground directional overcurrent elements, as are found in modern line reclosers
- additional relay functions that are not always found in line reclosers, including negative-sequence unbalance, overvoltage, undervoltage, and intelligent fuse-saving overcurrent
- PulseClosing technology that recloses for only one-half cycle to "test the line" (McCarthy and Staszesky 2008). Normal reclosers or breakers will reclose for several cycles, until they trip again on overcurrent.

When a device recloses, any downstream DER must be off-line beforehand. Otherwise, the phase angle differences on both sides of the device will cause high currents—even higher than fault current levels. These high currents can damage switchgear, transformers, motors, and the DER. IEEE 1547 requires that DER be off-line before any upstream utility device recloses. Such downstream DERs are in an electrical island. In some cases, the utility recloses faster than 2 s, which requires the DER to be off-line earlier than the 2 s allowed in IEEE 1547 for islanding detection. If the DER cannot do this, the utility might increase the reclosing time beyond 2 s, which adversely affects other customers, or DTT might be required, which

adversely affects the DER owner. A more flexible solution is to apply voltage restraint, which prevents automatic reclosing when the downstream voltage is higher than 10% to 20% of normal. If the downstream DER is off-line earlier than 2 s, reclosing would be automatically permitted. PulseClosing might provide another option for quick reclosing, because it limits the magnitude and duration of high currents that flow during a failed reclose.

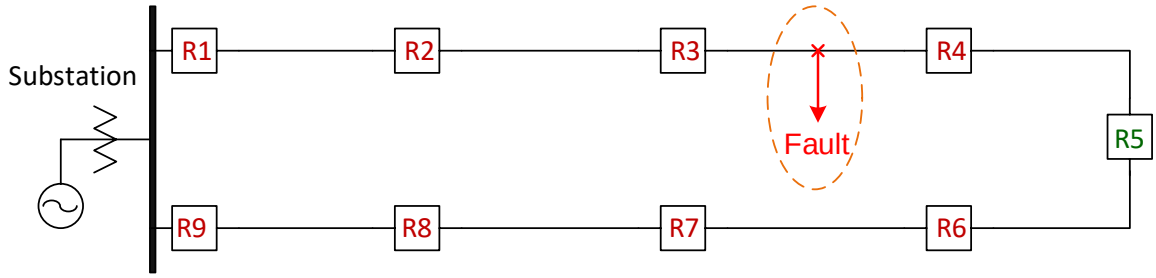

Figure 1.10. Autoloop Scheme without DER; **Red** Reclosers are Closed, **Green** Reclosers Are Open

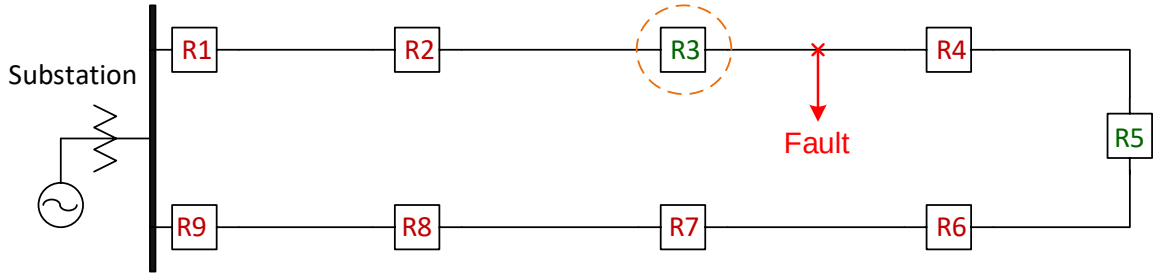

Figure 1.11. Autoloop Scheme without DER: Open R3 to Isolate the Fault

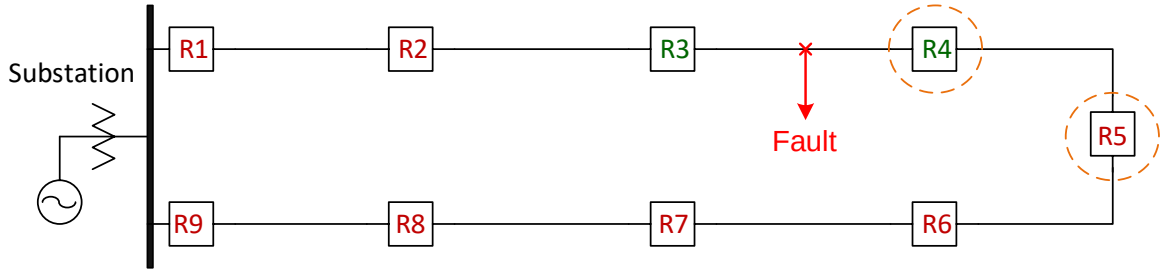

Figure 1.12. Autoloop Scheme without DER: Service Restored, except Between R3 and R4

Products are available that compete with the IntelliRupter for protection and automation (e.g., SEL-651R Advanced Recloser Control), although these do not include the half-cycle PulseClosing feature. Many utilities now require an advanced recloser control at the point of common coupling (PCC) for DER above a certain size threshold, instead of the simpler relays (e.g., SEL-547) that provide only functions mandated in IEEE 1547.

Autoloop protection schemes apply peer-to-peer communication between reclosers to (i) isolate a fault between the nearest upstream and downstream protective devices, and (ii) when possible, provide automatic restoration to customers downstream of the fault by closing normally open switches to back-

feed those customers from adjacent distribution feeders. These schemes have been demonstrated to provide significantly improved reliability in utility deployments (Glass et al. 2016; Starke et al. 2017).

By including communication between protective devices, these schemes eliminate a major disadvantage of classical time-overcurrent distribution protective coordination: that upstream devices will take longer to trip for a given fault current than downstream devices. This longer trip time results in the feeder being subjected to more damaging fault energy for faults in the more upstream portions of the feeder.

Although not strictly a part of autoloop protection schemes, current manufacturer implementations include the ability to limit the fault energy supplied to the feeder during fast operations when the protective device attempts to determine whether a fault has cleared or not. This is accomplished by closing the switching element briefly near the zero crossing of the voltage waveform.

1.6 Existing Practices – Secondary Networks

Figure 1.13 shows part of a secondary network in a downtown urban area, in which a three-phase, 208-volt network is served from six medium-voltage radial feeders. If there is a fault on the low-voltage side, fuses or cable limiters (a type of fuse) will clear it before any network protector (NWP) trips. Blown fuses and limiters must eventually be replaced, but there is enough redundancy on the low-voltage side that this does not have to occur immediately. This improves the service reliability, because there are still active cable paths to each secondary network load, and all of the primary feeders are still in service. If there is a feeder fault on the primary, its breaker opens as usual, while the two back-feeding NWPs open quickly on reverse power flow. The secondary network loads experience no interruption in service, even after several simultaneous contingencies on either the secondary or the primary. The main feature of this design is its high service reliability, without the expense of transfer switches.

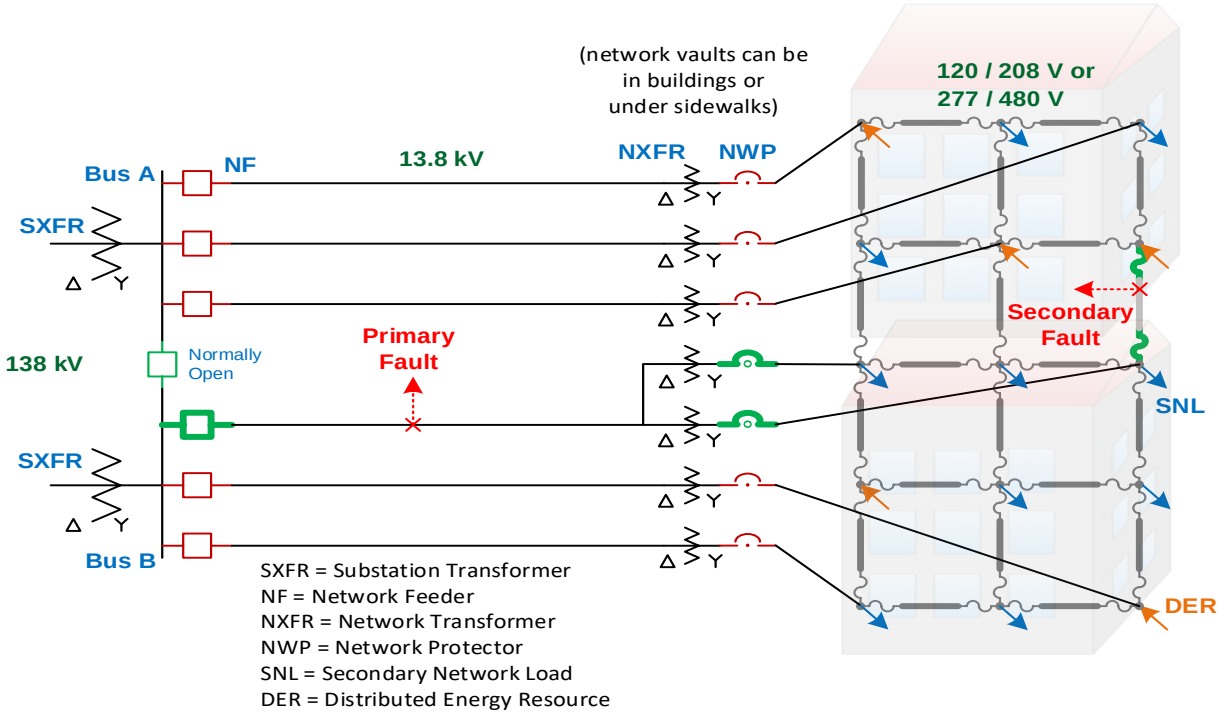

Figure 1.13. Secondary Spot Network with Primary and Secondary Faults, Cleared by Green ElementsOpening of the NWP on reverse power flow is an essential for service reliability,

but it has limited the penetration level of DERs connected to such secondary networks. No reverse power flow can be allowed through the NWP during normal operation. Existing practice is to limit DERs so that reverse power flow is essentially impossible, either at the building, facility, or network level (IEEE 2011). This precludes high-penetration DER on secondary networks.

NWPs are the major protective devices in secondary networks. Some cables also have cable limiters (fuses) to limit thermal damage to the cables under fault conditions. Typically, an NWP consists of a protective relay (or relay set), a controlled circuit breaker, and a number of contacts. It is connected between each network transformer and the associated collector bus (a single bus banking all the secondary sides of the network transformers connecting to a customer). Almost all NWPs are designed to trip when they detect reverse power flow, in order to prevent back-feeding power from one transformer through another. As a result, direct integration of distributed generation into the secondary network is limited in current utility practice.

The network protector relay (NWPR) is the "brain" of an NWP. It senses the back-feeding power flow by comparing the magnitude and phase angle differences between the network transformer voltage, the collector bus voltage, and the corresponding current. It is set to close when the transformer is to supply power to the secondary network, and automatically open the circuit breaker when the network back-feeds power to the primary feeders. The relay is also responsible to reclose the circuit breaker when predetermined electrical conditions on the feeder and the secondary network are met. The relays are set to trip the NWP (Baier 2003) when detecting

- a fault on a primary feeder, before the primary feeder breaker can open
- a fault on a primary feeder, after the primary feeder breaker has opened
- a fault in a network transformer connected to the subject NWP
- an open primary feeder breaker, even if there is no fault on the feeder.

The NWP must also coordinate with fuses, leading to a fast trip for high-current faults on the primary feeder or in the network transformer.

Selectivity is especially important. The NWP must not trip for any type of fault in the low-voltage portion of the network, nor during any faults on adjacent primary feeders or adjacent network transformers.

The first application of NWPs, developed by Westinghouse Electric and Manufacturing Company, can be traced back to 1922. Since then, the protector relay technologies have advanced from electromechanical to solid state, and now microprocessor based. Electromechanical relays were extensively produced and widely installed until the 1960s. They still have a large installation base. Solid-state and microprocessor-based relays were introduced in the mid-1960s and late 1980s, respectively, replacing the old electromechanical relays used in NWPs. Microprocessor relays have evolved into a second generation (e.g., Eaton Microprocessor Communications Variant, MPCV), from the first-generation products (such as Westinghouse Microprocessor Controlled Relay, MPCR). Since GE left the network protector and relay business in 1982, the major vendors in the current market include Eaton, ETI/Richards Manufacturing, Schweitzer, and Digital Grid.

Table 1.2 lists some of the representative NWP products from these vendors and their characteristics.

Table 1.2. Summary of Network Protector Products

Model	Vendor, Brand Name	Product Type	Function and Characteristics
CM22	Eaton, Cutler Hammer	NWP	- Since 1934 - Still manufactured - Newer products such as CMR-8 (1975) and CMD (1991)
CM52	Eaton, Cutler Hammer	NWP	- MPCV sequence based, both straight line and circular close characteristics
CNJ, CN33	Westinghouse	NWPR	- Electromechanical - Watt directional trip characteristics
ID-2	GE	NWPR	- Electromechanical
MPCR	Westinghouse	NWPR	- First-generation microprocessor relay - Sequence based (positive) - Watt and watt-var sensitive trip - Only straight-line close characteristics
MPCV	Eaton	NWPR	- Second-generation microprocessor relay - Sequence based (positive) - Watt and watt-var sensitive trip - Both straight line and circular close characteristics
MNPR	ETI/Richards	NWPR	- Solid state - Direct replacement for old electromechanical or solid-state relays - Power based using either actual or nominal voltage magnitudes - Watt directional trip characteristics
SEL 632-1	Schweitzer	NWPR	- Power based using nominal voltage magnitudes - Watt directional trip characteristics
DG-6000/6001	Digital Grid	NWPR	- Either sequence based or power based - Watt directional trip characteristics

1.7 Existing Practices – Microgrids

Microgrids have existed for over 100 years, and protection schemes for microgrids supplied from local synchronous generation are well understood. The same principles apply when that kind of microgrid operates in parallel with a single, strong utility source. Problems arise when inverter-fed microgrids need to operate in either utility-connected or stand-alone configuration. The disparity in fault current levels between these modes makes it difficult to set overcurrent relays (Haron et al. 2012). Recent suggestions have included a supplemental source of fault current for microgrid mode, or directional comparison relaying with cascading time delays (Hatziargyriou 2014). The first idea creates a new single point of failure for the whole protection system, and the second idea produces longer and longer fault clearing times. Both may increase equipment damage until the fault is cleared.

Figure 1.14 shows directional overcurrent protection of a microgrid when there is enough difference between fault current and load current to operate directional overcurrent relays. However, the fault current magnitude does not vary much with location, because the circuit impedances are small, and therefore, time-overcurrent coordination will not work. Instead, each breaker/relay pair has a definite time delay to trip after fault current is detected, and these settings are labeled on each breaker. Most of the time-delay

settings are different in the forward and reverse directions. In Figure 1.14, on the main loop, the clockwise directional delays are **green** and the counterclockwise directional delays are **blue**. Within each switchboard (SWB), the inward directional delay is **green**, and the outward directional delay is **magenta**.

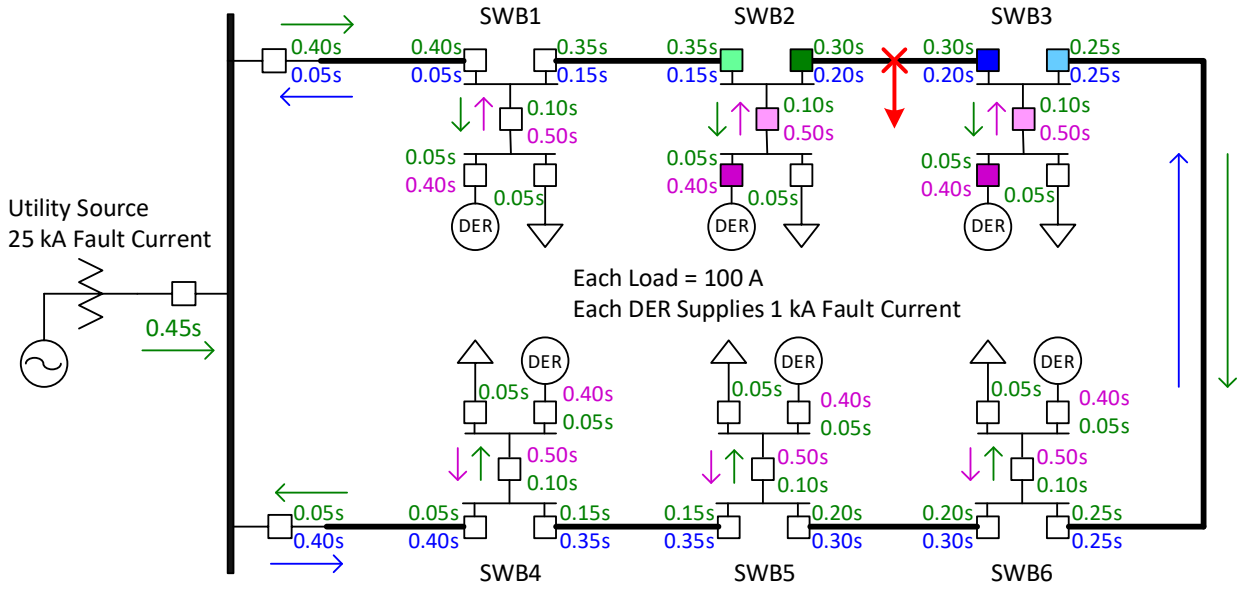

Figure 1.14. Directional Overcurrent Microgrid Protection Example

Suppose a fault occurs at the **red** location in Figure 1.14. If the utility source is connected, the fault current should exceed 20 kA. If the microgrid is islanded with one DER, the fault current should be 1 kA, which is still higher than the maximum steady-state load current of 600 A through any breaker. We could set the fault current threshold at 800 A. Whenever the utility or additional DERs are connected, it would be desirable to increase the fault current threshold, allowing more margin for load dynamics. In any case, all relays should detect the fault, but the time delays determine which ones operate. The **dark blue** breaker at SWB3 should trip in 0.20 s and the **dark green** breaker at SWB2 should trip in 0.30 s. If the primary breaker at SWB3 fails, then the secondary breakers at SWB3 need to trip, the **light blue** one in 0.25 s and the **dark magenta** one in 0.40 s. If the primary breaker at SWB2 fails, then the secondary breakers at SWB2 need to trip, the **light green** one in 0.35 s and the **dark magenta** one in 0.40 s. If either DER breaker fails to trip, the corresponding **light magenta** breaker should trip in 0.5 s. If secondary breakers fail to open on the main loop, there are additional backup breakers in each direction that should operate at longer time delays.

For any fault at a different location, we can verify that the scheme is selective, i.e., the least possible amount of load or DER is disconnected while isolating the fault.

- Faults within a load or DER should be cleared at the SWB within 0.10 s, without opening any breaker on the main loop.
- Time delays on the main loop coordinate in both clockwise and counterclockwise directions.
- Race conditions may occur on the main loop, but then it does not matter which relay wins. For example, if the **light blue** breaker at SWB3 has to trip in 0.25 s for a fault at the **red** location, the breaker on the other end of the cable at SWB6 would also trip in 0.25 s, i.e., on its **blue** setting, because the fault location is counterclockwise from SWB6. With no load between SWB3 and SWB6, and no fault on that cable, it does not matter which end trips first. We could eliminate the race conditions with longer time delays, but that would increase fault clearing times.

- The utility breaker relay is shown with a long directional time delay of 0.45 s to coordinate with the feeder/microgrid relays. If there is a fault between that breaker and utility source, any connected DER would back-feed the fault. Such faults on the utility source would be detected with transformer differential, bus differential, and/or line protection relays not shown on Figure 1.14.

Once a fault has been cleared, the time-delay settings should still work for subsequent faults, but they may no longer be optimal. An adaptive relay setting scheme would change the fault detection thresholds and time delays depending on which sources are connected and which circuit segments are in service. If the system is left with only inverter-based DERs after disconnecting the utility source, there probably will not be enough fault current to operate a directional overcurrent scheme.

Microgrid protection is made challenging by both the presence of DERs and the ability of microgrids to island. Microgrid protection can be divided into two regimes: (i) microgrids with fault-capable DERs, such as synchronous generators, and (ii) microgrids without fault-capable DERs, such as inverter-interfaced generation. Microgrids with fault-capable DERs introduce several potential issues into a distribution system. These include

- blinding of protection or desensitization, similar to Figure 1.4: DERs downstream of protection will contribute to the fault current, so the amount of fault current measured by the protective devices is reduced.
- false/sympathetic tripping, similar to Figure 1.6: DERs on Feeder B can contribute to faults on adjacent Feeder A, causing the breaker on Feeder B to trip.
- recloser/fuse miscoordination, similar to Figure 1.3 and Figure 1.5: Fault current contribution can increase fault current outside the range in which fuse and recloser coordinate, so the fuse blows before the recloser fast-trips. The worst case is when both the fuse and the fault are behind the recloser. The fuse now sees higher fault current than the recloser, and the fuse is even more likely to blow before a recloser fast operation.
- fuse-fuse miscoordination.
- failed auto-reclosing.

For DER operating outside of a microgrid, these issues can be overcome by adding breakers at the generator output terminals. For microgrids, however, this is not a desirable approach, because microgrid generation must be kept online in case the microgrid is required to island (Choudhary et al. 2014). This creates two difficulties for design of a protection scheme: (i) the electrical configuration of the network has changed, and (ii) microgrids are commonly designed with inverter-interfaced generation that does not provide fault current (Tecogen 2018).

Current research in microgrid protection focuses on addressing the challenges of bidirectional power flow, lack of fault current, and being able to operate under both grid-connected and islanded conditions. Topic areas for inverter-interfaced microgrid protection research are summarized in Choudhary et al. (2014) and Memon and Kauhaniemi (2015). These methods can be divided into the following classes:

- directional overcurrent (Sharaf et al. 2018)
- voltage based: direct-quadrature transform (DQ0), total harmonic distortion (Al-Nasseri and Redfern 2008, Al-Nasseri et al. 2006)
- differential (Nikkhajoei and Lasseter 2006, Dewadasa et al. 2011, Kar and Samantaray 2014, Sortomme et al. 2010)
- impedance (Dewadasa et al. 2008a, 2008b, 2009)

- adaptive (Perera and Rajapakse 2006, Saleh 2014, Voima et al. 2011)
- current traveling wave (Li et al. 2014, Shi et al. 2010)

These schemes are described in more detail as follows.

An approach to protection of inverter-interfaced microgrids using existing technology is described in Nikkhajoei and Lasseter (2006), where the protection scheme mainly focuses on line-to-ground and line-to-line faults. This protection scheme assumes that the fault current provided by generation is less than or equal to 200% of the rated current. The approach assumes that the maximum load power imbalance is 20%, and relies on thresholding the negative and zero-sequence current to detect faults. Backup protection is provided via time-overcurrent relaying, which also detects three-phase faults. The main limitations of this method are that (i) it can misoperate under unbalanced load conditions, potentially cutting power to critical loads, and (ii) it will operate slowly for three-phase faults, because it relies on backup protection for this.

Sharaf et al. (2018) propose a directional overcurrent approach. This method does not have the strict time-synchronization requirements of differential protection, but it does require fault current to operate.

In Al-Nasseri et al. (2006), a protection method is proposed that makes use of the DQ0 transform to detect line-to-line and line-to-ground faults based on an increase in the deviation of the quadrature voltage from a reference value, typically measured at the utility point of common connection. This method does not require the presence of fault current, and is suitable for microgrids with inverter-interfaced generation. It is not clear how the reference voltage is generated during islanded operation, however. The same authors present another method based on the voltage total harmonic distortion. This method is only suitable for protection of generation, not lines or buses (Al-Nasseri and Redfern 2008).

A collection of related methods utilizes line admittance for fault detection, which overcomes the issue of lack of fault current in inverter-interfaced microgrids (Dewadasa et al. 2008a, 2008b, 2009). This collection of methods still has some problems with selectivity, which introduces complexity in application.

Two methods are proposed that locate faults based on wide-area protection schemes that monitor currents on each line in the microgrid. One such method relies on dividing a microgrid line into segments with protective devices (Voima et al. 2011). Each device can measure voltage and current, and all devices are connected via a high-speed communications link via IEC 61850 (IEC 2019). Fault detection has two stages:

1. detecting the presence of a fault when an undervoltage occurs
2. locating the fault between the two closest protective devices at which the current changes sign.

The two protective devices surrounding the fault will open to isolate it. This method has the advantage of not being reliant on fault current, but introduces the complexity of centralized communication and control.

In Saleh (2014), another method is tested in laboratory conditions that does not require voltage sensing nor high-speed communication. The proposed method uses the wavelet packet transform of the DQ0 transform of the sum of sensed currents at each node of the microgrid. This method can avoid misoperation during switching transients. However, it requires centralized communication and coordination to locate faults. It also requires fault current, which precludes its use for microgrids with inverter-interfaced generation.

A similar method is proposed in Perera and Rajapakse (2006). It uses the discrete wavelet transform to generate coefficients for the current sensed at the endpoints of each line flowing into a node in the system. Detecting the polarity of the wavelet coefficients makes it possible to isolate the faulted bus or line. The method is suitable for meshed microgrids with distributed generation, but given its lack of voltage sensing, also requires fault currents in order to detect the presence of a fault.

Traveling-wave protection relies on detecting the current wave fronts that propagate on a distribution line after a fault occurs (Li et al. 2014, Shi et al. 2010). This protection method does not require voltage sensing, but it does require the following:

1. sensing at both ends of lines, to verify that a fault occurred on the protected line and not elsewhere in the system.
2. time synchronization of all devices on the system.
3. a fast sampling rate of at least 500 kHz.
4. global communication and coordination to locate faults on a meshed system.

Differential relays for protection of microgrids are proposed in Dewadasa et al. (2011). This approach is recommended over others in Conti et al. (2009) for microgrids with inverter-interfaced generation. This approach is secure in that it protects against line-to-line and line-to-ground faults, including high-impedance faults, and operates quickly, with good selectivity and sensitivity. Additionally, it works for both grid-connected and islanded operation. Backup protection and protection against three-phase faults are provided by undervoltage and overcurrent protection, or by using communication to send a trip signal to relays at the same bus. This approach requires time synchronization between relays at either end of a protected line, especially for long lines, and requires relays at each line tap (Dewadasa et al. 2011, Sortomme et al. 2010). In the case of Sortomme et al. (2010), global low-latency communication is required, but the authors claim that time synchronization is not necessary. In Kar and Samantaray (2014) and Samantaray et al. (2012), the authors loosen the requirements for time synchronization with differential methods by comparing the signal energy of the S-transform of the current measurements, where the S-transform is a form of wavelet transform that preserves phase information.

1.8 Summary of New Challenges

Over the next one to five years, increasing penetration of DERs and microgrids will create new protection challenges in five areas:

1. Mixtures of rotating-machine and inverter-based DERs will complicate the detection of unintentional islands. Rotating machines can resemble the utility grid too closely for the built-in inverter islanding detection methods to work properly. These are currently tested only for single inverters connected to the grid. In a realistic scenario with many inverters of different makes and sizes, it would also be difficult to detect islanding, because the built-in algorithms can work against each other. One example would be islanding in which one inverter tries to increase the grid frequency while another inverter tries to decrease the frequency; the result could be that the grid frequency does not shift, so the island would not be detected.
2. Inverter-based DER acts like a voltage-controlled, positive-sequence current source, with little or no zero-sequence or negative-sequence content. Rotating machines in DER act like voltage sources, much like the grid itself. The behavior of rotating machines on the grid is well understood; simplified fault current models are available, with dynamic and transient models also available if needed. The rotating models, software tools, and machine type tests, which are the basis for model parameters, have evolved together over more than 100 years of operating experience. Inverters are much newer

and very different from rotating machines; they do not provide much fault current, they can follow the terminal voltage angle very quickly, and there are no standard type tests for simplified fault models. This makes it harder to perform protection analysis, and increases the chance for errors.

3. The default undervoltage trip settings in IEEE 1547 have changed. Presently, the most significant setting for fault detection is the undervoltage trip within 0.16 s when the voltage drops below 50%. The proposed revision defines three categories of DER for undervoltage trip. The first two categories have a default trip within 0.16 s when the voltage drops below 45%, which is a little less sensitive than in the current standard. More importantly, Category III, intended to apply to "very high penetration" of DER, has the default trip within 2.0 s when the voltage drops below 50%. That is likely to increase the fault detection time for DERs that presently detect faults by undervoltage. There are ranges of adjustability to these settings, and several other settings to consider as well, in the new IEEE 1547-2018. These changes enable DER ride-through, but they also complicate system protection.
4. Microgrids can operate in, and transition between, different modes, including grid connected, intentionally islanded after separating from the grid, and black start (sometimes called grid forming). Each mode calls for different control responses to maintain voltage and frequency. The available fault current magnitudes and directions also change significantly between modes. In a normal utility protection study, the fault currents at a given location change with different system configurations, but usually within a range of two-to-one. With relatively few exceptions, one relay scheme and one relay settings group work well for each location. This is not true for microgrids, because the strengths and types of sources vary much more; the protection schemes and settings need to be more adaptive.

Overcurrent relays only need current transformer (CT) sensor inputs, but directional overcurrent relays also need voltage transformer (VT) inputs to determine phase angle (i.e., direction) of the current with respect to voltage. VTs are also needed for distance relays and many other types of relays. If the voltage drops too low during a fault, the VT output can be too low for the phase angle to be determined, which leads to loss of directionality. This can be mitigated inside the substation, but it is harder to deal with out on the feeder, including at DER locations. This is one example of how new relaying schemes could increase the requirements for distribution system sensors.

2.0 Metrics for Evaluation

When a utility engineer designs the protection for a distribution system, the devices, algorithms, and settings are specified to achieve the goals of dependability, security, sensitivity and speed. Cost might be included as a metric, but is not usually a major factor when the communications infrastructure is already in place. Utilities may use lists of preferred vendors and relays, and the cost of protection is a small percentage of total system cost. However, in proposing brand new protection schemes, cost must be included along with the basic protection metrics. Any new workforce training requirements should also be included in the cost. Engineers might have to write and test custom programs for digital relays, which would also incur a cost.

In the context of research aimed at solving bidirectional power flow issues in the near term, two more metrics become important. First, flexibility should be considered, because any new protection scheme should allow more bidirectional power flow on the distribution system. Second, technological maturity should be considered, because we need to choose functions that are available in commercial products or that could be quickly developed.

For interruption devices and relays commonly used on distribution systems, the following vendors have a significant presence:

- reclosers: Eaton, G&W Electric
- relays and recloser controls: Schweitzer, GE Multilin, ABB, Siemens, Beckwith, Basler
- network protector relays: ETI/Richards, Eaton, Schweitzer, Digital Grid
- instrument transformers: ABB, GE, many others

Table 2.1 summarizes and categorizes the quantitative evaluation metrics that are used in the remaining sections of this report.

Table 2.1. Evaluation Metrics for New Protection Schemes

Metric	Category	Criterion or Quantity
1	Dependability	Must detect all faults within the protected zone; **failures are disqualifying**.
2	Security	Must not trip for any fault outside the protected zone; **failures are disqualifying**.
3	Selectivity	Must trip the minimum number of devices to isolate the fault, after any reclosing activity has completed. Primary protection must trip before backup protection. **Failures are disqualifying**.
4	Sensitivity	Maximum ground fault resistance before the scheme fails to operate for a ground fault. This can be presented in the form of a graph of resistance vs. fault location.
5	Speed	Time between fault inception and a relay command to trip. This can be presented in the form of a graph of time vs. fault location for different types of fault.
6	Cost (Equipment)	Expected purchase, design, and installation costs for all relays and sensors, per feeder, including both utility-owned and DER relays for a high-penetration case.
7	Cost (Communication)	Expected purchase, design, and installation costs for new communications infrastructure, per feeder, to support the new scheme. Significant communication costs are disqualifying for now.
8	Cost (Labor)	Expected training and engineering costs for a new scheme, per utility, consulting, or DER organization.
9	Flexibility	The highest DER penetration level, defined as DER Capacity/Peak Load, for which no disqualifying failures occur.
10	Maturity (TRL)	The Technology Readiness Level of commercial products that could implement the new scheme.
11	Maturity (Market)	The number of vendors that currently supply products that could implement the scheme.

3.0 Technical Approach to Evaluation

For the near term, our attention focuses on technologies that have successful commercial implementations, and that do not require extensive communications infrastructure. For transmission lines, time-domain (incremental) distance protection and single-point traveling-wave protection have been demonstrated (Schweitzer and Kasztenny 2017). A focused directional relaying scheme has also been demonstrated for industrial facilities with DERs that are served from radial feeders (Hartmann 2017). There are important differences between the demonstrated applications and our application of feeder-connected DER, but some combination of these functions could be successful. If so, we believe the vendors could develop new products within a year, because the underlying components have already been developed.

Some distribution systems have access to communications, but these usually lack enough reliability and bandwidth for protection applications. For example, IEC 61850 (IEC 2019) specifies that Generic Object-Oriented Substation Event messages need to be grouped and transmitted within 4 ms. A communication system that was installed for advanced metering infrastructure (AMI), integrated volt-var control, and/or distributed energy resource management may take seconds to minutes for transmission, with no guarantee of delivery. This performance is not adequate for protection.

The cost of protection increases significantly when communication is added. For example, the communication cost per meter for 12 large-scale AMI deployment projects ranged from $8 to $205, averaging $65 per meter (OE 2016). For communication-assisted protection of distribution systems with DER, the purchase cost per terminal for a spread-spectrum radio transceiver begins at about $1000, which translates to a few thousand dollars installed (Schweitzer et al. 2012). Spread-spectrum works over distances up to 20 miles with direct electromagnetic line of sight between stations. However, if repeaters and towers are needed, or fiber optic communications are used instead of spread-spectrum communications, the cost increases to the point where $600 K is a typical planning figure for new DTT links (PG&E 2018). The high-end example of $205 per meter for AMI deployment included fiber, which provides an example of how the extra cost of fiber optic communications could be amortized for DER protection.

Given 5 to 10 years, more advanced protection systems could be feasible, including those that rely on high-speed communications. However, the rapid growth of DERs and the publication of IEEE 1547-2018 call for solutions within one or two years.

3.1 Modeling Tools

For this report, protection schemes will be assessed using an electromagnetic transient simulation program called Alternative Transients Program (ATP), and a general modeling program called MathCAD (Dusang and Johnson 2008). The IEEE 13-bus (Kersting 2001) and 500-node (Arritt and Dugan 2010) radial test feeders are modeled in ATP. ATP simulates current and voltage waveforms during a variety of system conditions and fault events. The IEEE test feeders are publicly documented (DSASC 2019) and widely used by researchers, which fosters replicability of the results presented later. Once the model has been built, ATP can be scripted for efficient parameter sensitivity studies. ATP exports the waveforms in COMTRADE format (IEEE 2013), which is one of the formats used for open-loop hardware testing of relays.[1] Therefore, the approach and models presented in this report can be adopted later for laboratory

[1] The MathCAD worksheets import COMTRADE files, filter the waveforms into phasor components, and interactively display the results of different sensing and logic functions within a relay. Once the COMTRADE file

testing. The model files can also be made available to licensed users of the respective simulation tools, none of which are open source, through a mechanism still to be determined.

Figure 3.1 shows the ATP model of an IEEE 13-bus system, used to evaluate the incremental and focused directional functions. This system is unbalanced, with a mixture of three-phase, two-phase and one-phase lines and loads. In converting the data from power flow simulation to transient simulation, all loads were made constant impedance, and the substation transformer taps were fixed to maintain acceptable voltage under peak load. The lines were modeled with constant-parameter, traveling-wave components instead of lumped impedances. These changes were appropriate and necessary because the original power flow data emphasizes non-linear load behavior and transformer tap changes over long time frames, while the ATP data emphasizes high-frequency behavior over very short time frames.

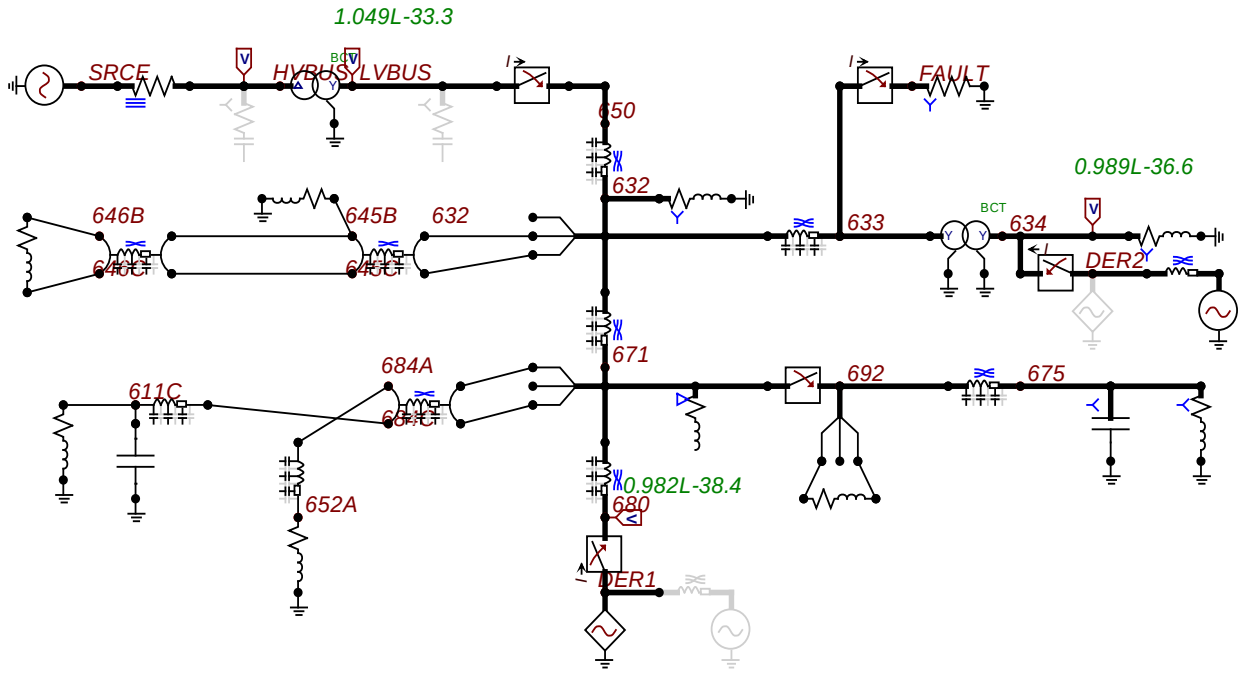

Figure 3.1. ATP Model for Incremental and Focused Directional Relay Evaluation

For preliminary studies, two three-phase, 500 kVA DER units were installed at locations DER1 (4.16 kV bus, near the bottom of Figure 3.1) and DER2 (480 V bus, near the top right of Figure 3.1). This DER capacity represents about 28% of the feeder peak load; as such, it is only a starting point for high-penetration scenarios. At DER1, the Norton source configuration is shown with a diamond-shaped current source, while the alternative Thevenin voltage-source configuration is grayed out (i.e., disabled). At DER2, the converse applies. We actually ran the simulations with either both Norton or both Thevenin configurations enabled. There are three relay locations of interest:

1. at the substation feeder breaker, sensing current through the switch from LVBUS to Bus 650 and the voltage at Bus 650
2. at DER1, sensing current through the switch from DER1 to Bus 680 and the voltage at Bus 680
3. at DER2, sensing current through the switch from DER2 to Bus 634 and the voltage at Bus 634.

has been imported and filtered, MathCAD allows us to interactively define and explore new relay settings and functions. MATLAB and Python can also be used for modeling and plotting relay functions.

The simulation time step in Figure 3.1 is 1 μs, and the single-line-to-ground fault (SLGF) is applied at 66.67 ms (i.e., four cycles into the simulation) on Phase A at Bus 633.

Figure 3.2 shows a version of the 13-bus model for single-point traveling-wave simulation, with many of the branches and most of the loads removed. The same fault is applied at time zero of the simulation, with a time step of 1 ns, and the simulation ends at 40 to 200 ms. The simulation time is short to capture the traveling-wave arrivals and reflections caused by the fault; it is not intended to capture the peak fault current.

DER2 is not included because the transformer from Bus 633 to Bus 634 would severely disrupt the traveling waves from the high-side fault. We only expect a traveling-wave method to work when the DER and fault locations are at the same voltage level, as at DER1. Distribution feeders have many load-serving transformers tapped from the line, one of which is shown in Figure 3.2. The waves travel past this transformer, not through it. This example is a 100-kVA, single-phase center-tapped transformer, with a 100-kVA, 0.8 power factor aggregate load connected to the 120-volt side. For very short time periods, this transformer will mainly affect the traveling waves due to a small amount of inherent capacitance seen from the high side.

At the DER2 location in Figure 3.2, the Norton configuration is enabled with a parallel equivalent impedance. Even if the DER2 inverter acts as a controlled current source in steady state, as in Figure 3.1, some realistic impedance must be included in the model. Otherwise, traveling waves would encounter an open circuit at the controlled current source, which is not realistic. The shunt capacitance at the PCC represents a voltage sensor, with current monitored at the neutral end. Section 6 illustrates why this type of sensor may be optimal for the single-point, traveling-wave method on distribution feeders.

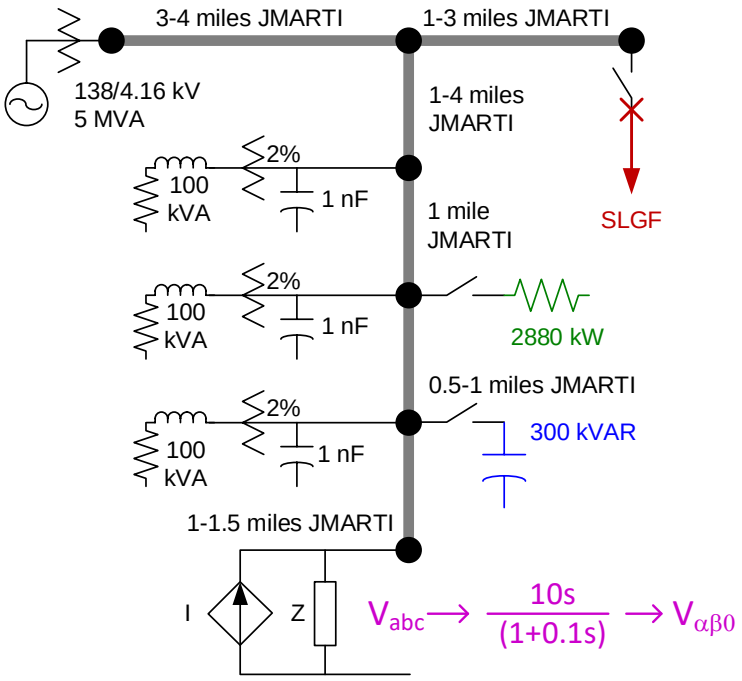

Figure 3.2. ATP Line and Transformer Models for Single-Point Traveling Wave

Figure 3.2 also shows in magenta that the voltage signals are processed through a low-pass filter, differentiator, and Clarke transformation to help detect wave arrival times (Schweitzer et al. 2014). That processing was part of the ATP model for this report, but it could also be done after simulation. The

voltage sensor design is important, because most available VTs lack adequate frequency response. The use of CTs has been suggested in order to use current waves instead of voltage waves, but the resulting wave signatures are not as easy to identify (Schweitzer et al. 2014). A capacitive voltage sensor has also been suggested, with a secondary current sensor connected at the grounded end of the capacitance. This kind of sensor would have adequate frequency response, but it represents an extra cost (Schweitzer and Kasztenny 2017).

3.2 Inverter Model

The inverter model was developed to mimic the behavior of a real single-phase inverter, in simplified form. First, block diagram logic was implemented to maintain real power output at the steady-state value, subject to a limit on the root mean square (RMS) value. Because of this, under low-voltage conditions, the inverter current increased to a limit of around 1.1 per unit. Second, a phase-locked loop (PLL) was implemented using a quarter-cycle transport delay for single-phase inverters (Teodorescu 2011). After any disturbance, the PLL acted to bring the output voltage and current in back in phase. This also had the side effect of appearing to control reactive power, but that was not the PLL's main purpose. We only wanted to obtain realistic results for the dynamic angle behaviors during fault conditions. A real PLL would provide the same function, but perform differently. The logic for both magnitude control and the PLL were used to drive a controlled current source component in ATP.

Figure 3.3 shows the voltage (**blue**) and current (**red**) for DER as represented by Thevenin (left) and controlled Norton (right) sources. In both cases, the prefault current and voltage are in phase, the fault occurs at about 0.167 s, and the post-fault voltage is about 0.46 per unit. The Thevenin source current, representative of a rotating machine, increases to about 6 per unit and the current lags the voltage by nearly 90 degrees. The controlled Norton source current, representative of an inverter, increases to about 1.1 per unit and the current lags the voltage for only one cycle (at most) and by less than 90 degrees. After that, the PLL brings the voltage and current back in phase.

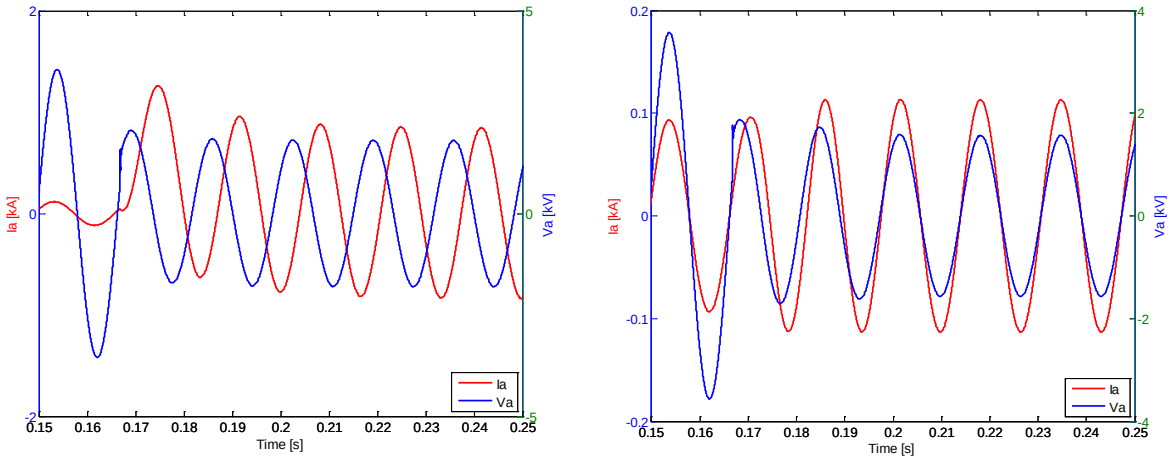

Figure 3.3. Thevenin (left) and Controlled Norton (right) DER Source Behaviors

4.0 Incremental Quantities for Radial Distribution

4.1 Principle of Operation

Incremental quantity protection is a variant of distance protection, which requires both voltage and current inputs to the relay (Schweitzer and Kasztenny 2017). These relays will have a reach, just like distance relays. On transmission lines, it is common to express the reach as a percentage of the protected line length. On distribution lines, which have many taps and branches within the protected zone, reach is better defined in terms of ohms, or in terms of distance to the fault with no taps or branches.

4.2 Analysis

Figure 4.1 shows the current and voltage waveforms at the feeder breaker for an SLGF on Phase A. Before the fault, we have some ratio of voltage to current, which defines a prefault impedance magnitude. That magnitude will vary as the load level varies, but the phase angle between current and voltage is also significant; before the fault, it will be closer to zero degrees, because loads are mostly resistive. After the fault, the current magnitude on Phase A increases by a factor of about 5, and the voltage decreases by about 1/3.[1] The impedance magnitude is much lower than it was before the fault. Equally important, note the sudden phase shift in Phase A voltage at the time of fault inception in Figure 4.1. The phase angle between current and voltage is closer to 90 degrees during the fault, because the source and line impedances are mostly inductive. However, this phase shift is not as pronounced as it would be on most transmission systems, because the X/R ratio on distribution systems is noticeably lower than that on transmission systems.

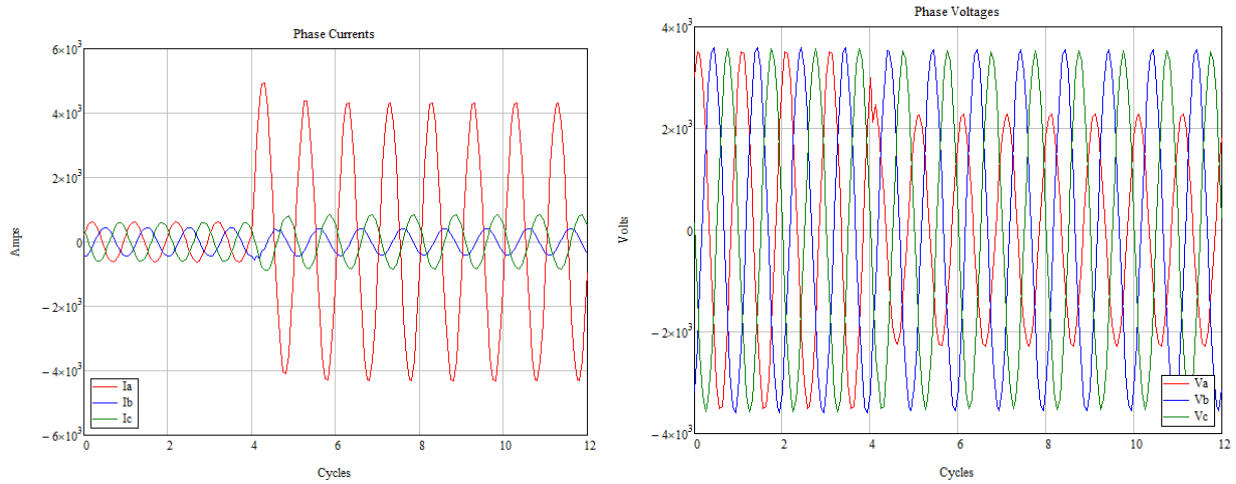

Figure 4.1. Substation Phase Currents (left) and Voltages (right) during SLGF with Thevenin DER Sources

Figure 4.2 shows the response at DER1 to the same SLGF on phase A. DER1 is assumed to be solar PV generation, represented by a current source. Therefore, the currents are not affected by the fault, but there

[1] All of the waveform plots in this report are instantaneous volts or amperes, not RMS quantities. In Figure 4.1, the nominal voltage is 4.16 kV line-to-line, or 2400 V line-to-ground, both RMS quantities. The instantaneous voltage peak in Figure 4.1 is expected to be approximately 2400 times the square root of 2, or 3394 V. This appears to be the case, except for relatively small voltage drops and unbalances between phases.

is still a significant voltage change at the time of fault inception, and thus a change in measured impedance at DER1. The case with a Thevenin source at DER1 (not shown) has an increase in current magnitude, similar to that in Figure 4.1, which would be representative of conventional sources like combined heat and power or landfill gas. Likewise, at DER2, the fault current responses are similar to those in Figure 4.1 or in Figure 4.2, depending on whether the source is Thevenin or Norton. The feeder breaker fault current response is always like that with a Thevenin source in Figure 4.1, although the magnitudes can vary slightly depending on the responses at DER1 and DER2.

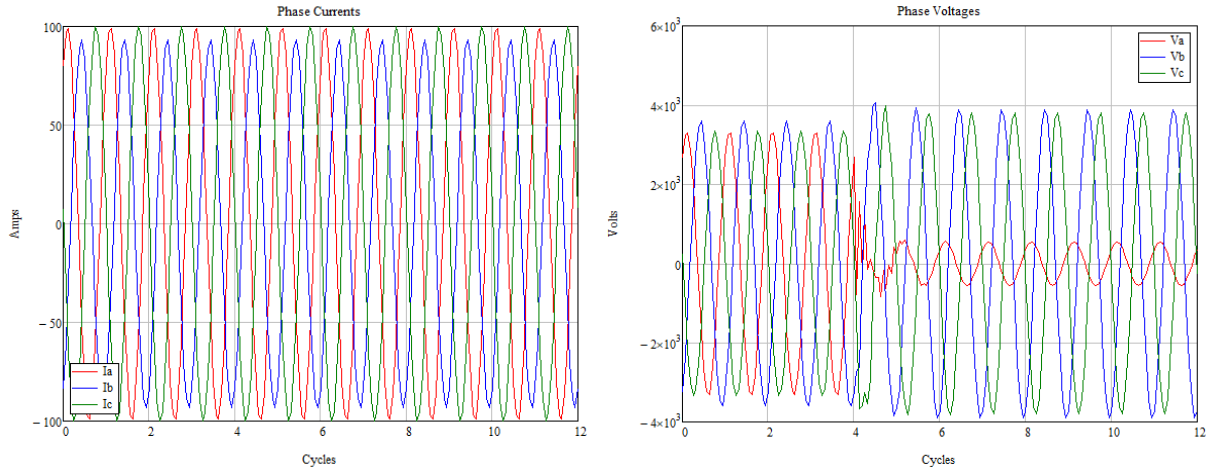

Figure 4.2. DER1 Phase Currents (left) and Voltages (right) during SLGF with Norton DER Sources

In the rest of this subsection, phasor magnitudes of the current and voltage responses will be presented, using waveforms that have been processed in MathCAD. Figure 4.3 shows these phasors for the waveforms in Figure 4.1. The MathCAD signal process takes about one cycle to initialize, and then shows the steady prefault conditions for up to four cycles. The vertical axis units are now RMS amperes and volts. The increase in current and the decrease in voltage begin at the fourth cycle, and have reached steady post-fault values within a cycle or two. The impedance magnitude on Phase A is approximately 1650 V/3100 A, or 0.53 Ω. Impedance magnitudes on the other phases are much higher, and a distance relay normally calculates three different ground impedances (A, B, and C) and three different phase loop impedances (AB, AC, and BC) to detect faults and identify their types.

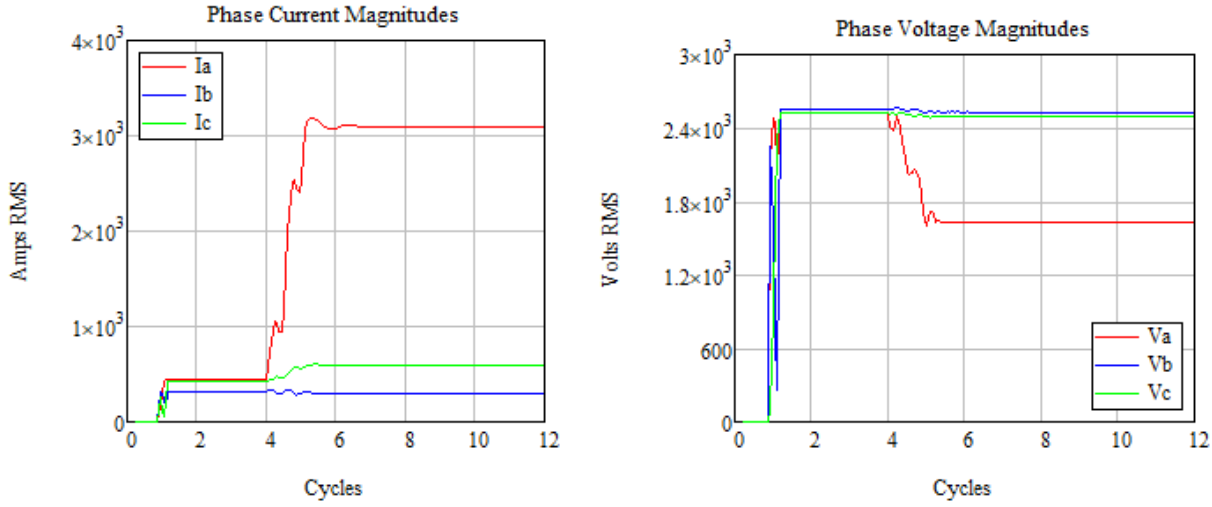

Figure 4.3. Substation Current (left) and Voltage (right) Magnitudes with Thevenin DER Sources

Figure 4.4 shows the phasor magnitudes at DER1 using a Thevenin source, and the post-fault impedance on Phase A is about 900 V/650 A, or 1.38 Ω. This is higher than for the substation source, but still detectable at DER1. Figure 4.5 shows the result at DER2 using a Thevenin source, and the post-fault impedance on Phase A is about 75 V/6800 A, or 0.01 Ω. This magnitude is much lower because DER2 is connected to a low-voltage system at 480 V. Furthermore, distance relays are not normally applied to see through transformers, but in this case, there is a detectable impedance change that might be considered useful.

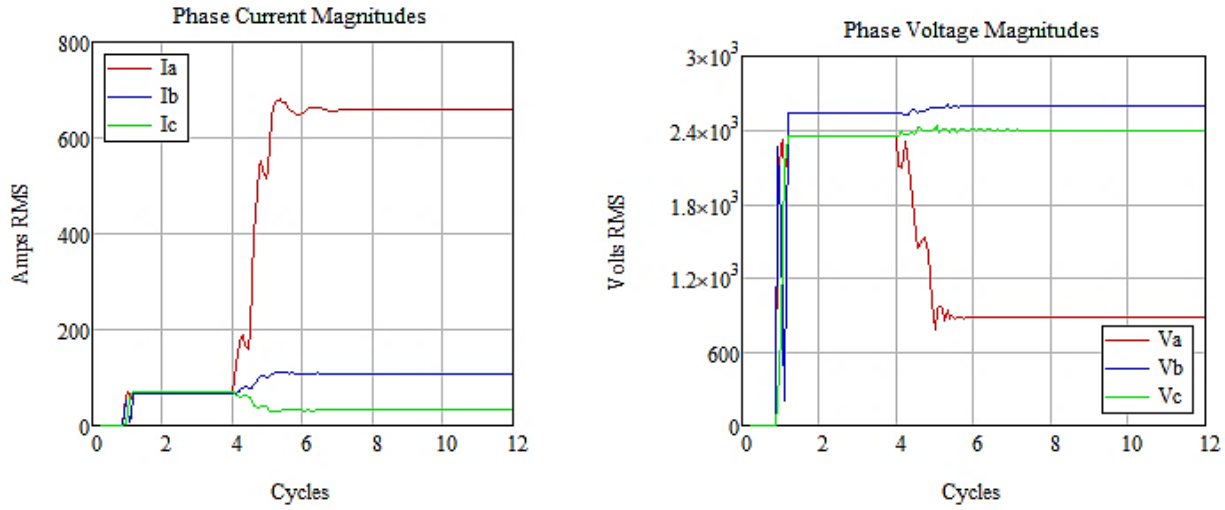

Figure 4.4. DER1 Current (left) and Voltage (right) Magnitudes; Thevenin DER Sources

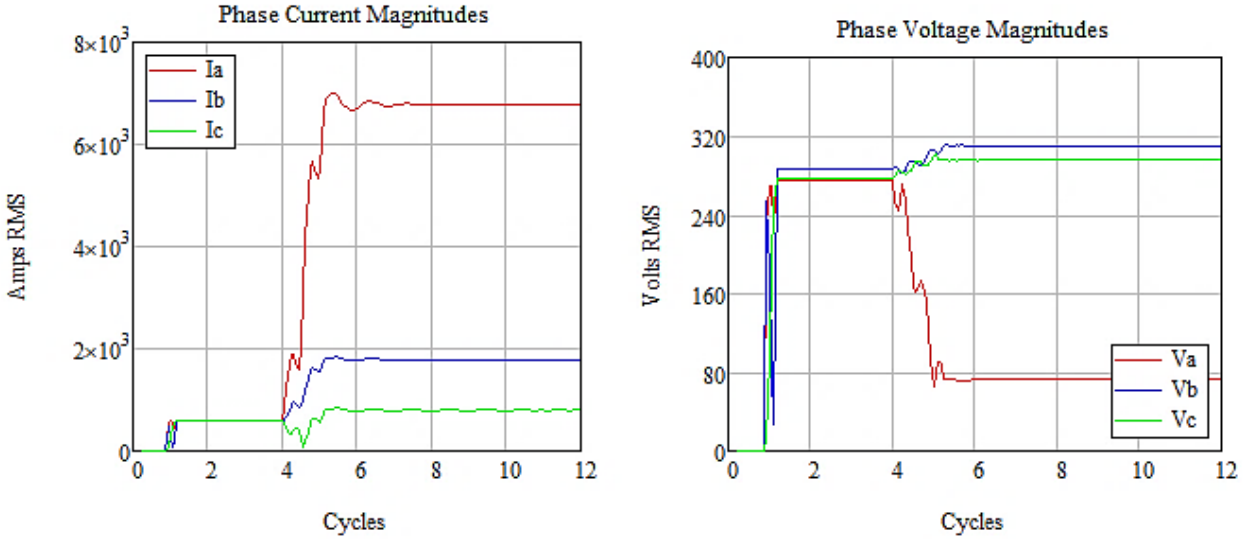

Figure 4.5. DER2 Current (left) and Voltage (right) Magnitudes; Thevenin DER Sources

Figure 4.6 shows the resulting phasor magnitudes at the feeder breaker for when both DERs are Norton sources (i.e., solar PV or batteries). These responses are similar to those in Figure 4.3, although the voltage magnitude is a little less with the Norton DER sources. The relay would operate properly in either case. Figure 4.7 and Figure 4.8 show the DER1 and DER2 current and voltage responses for when they are Norton sources. The current magnitudes do not change, because of the idealized source modeling, but there is still a detectable voltage drop. The problem with using voltage drop alone is that it cannot

distinguish between faults on the feeder connecting the DER, and faults on adjacent feeders or the nearby transmission system. In the new 2018 version of IEEE 1547, the DER should ride through faults if possible, unless the fault is actually on the DER's circuit.

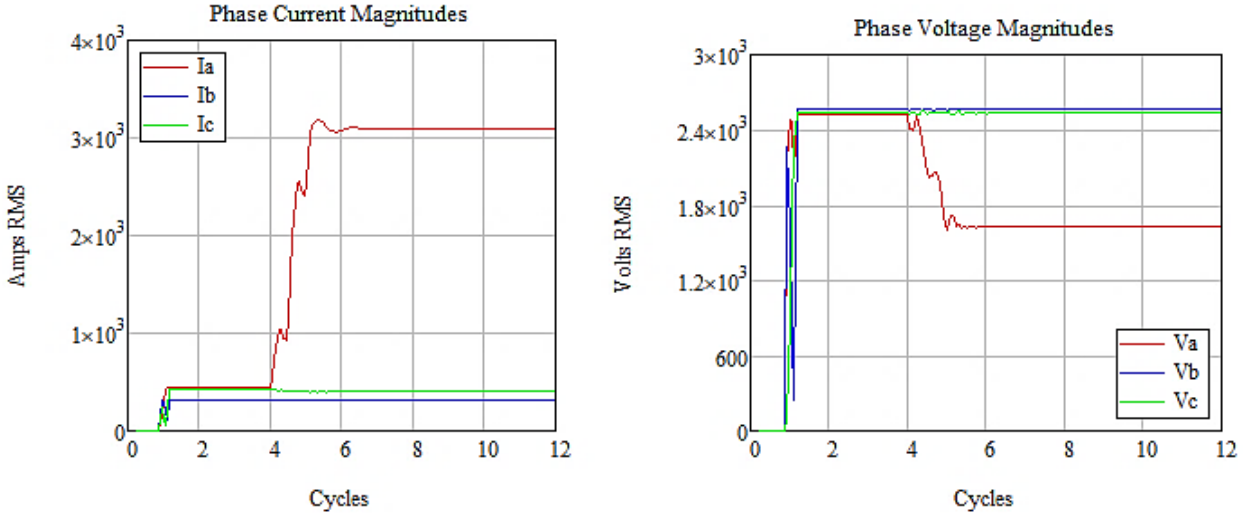

Figure 4.6. Substation Current (left) and Voltage (right) Magnitudes with Norton DER Sources

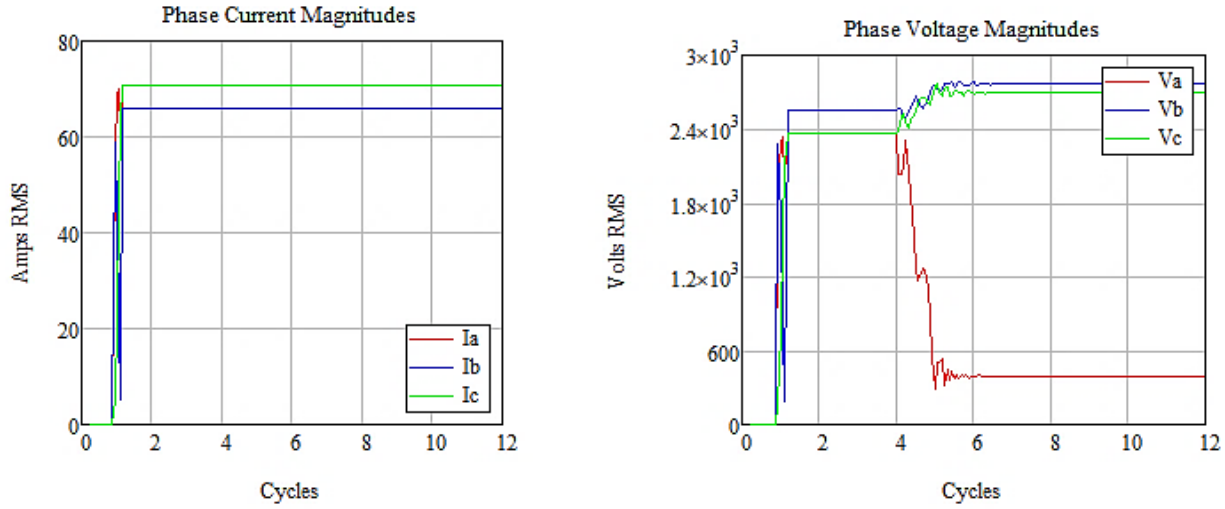

Figure 4.7. DER1 Current (left) and Voltage (right) Magnitudes with Norton DER Sources

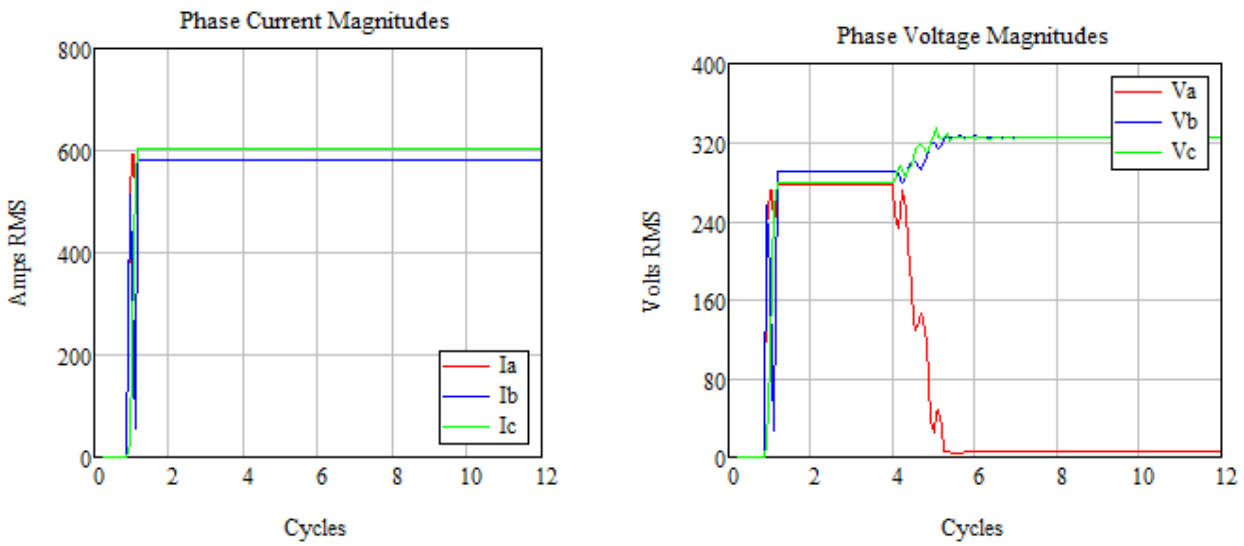

Figure 4.8. DER2 Current (left) and Voltage (right) Magnitudes; Norton DER Sources

Magnitude plots do not show the important influences of phase angle, both before and after the fault. Figure 4.9 shows the impedance plot at DER1, for both Thevenin and Norton source assumptions. This is a polar plot, with reactance, jX, on the vertical axis and resistance, R, on the horizontal axis, both in ohms. The positive-sequence line impedance from DER1 to the substation is about 0.94 + j 3.00 ohms, plotted as a blue line. Zone 1, the green circle, is set for 80% of the line impedance, and Zone 2, the brown circle, is set for 150% of the line impedance. The complex ratio between voltage and current is plotted as a red line, and it migrates from a normal loading condition toward the origin. Each sample impedance is marked with a red X.

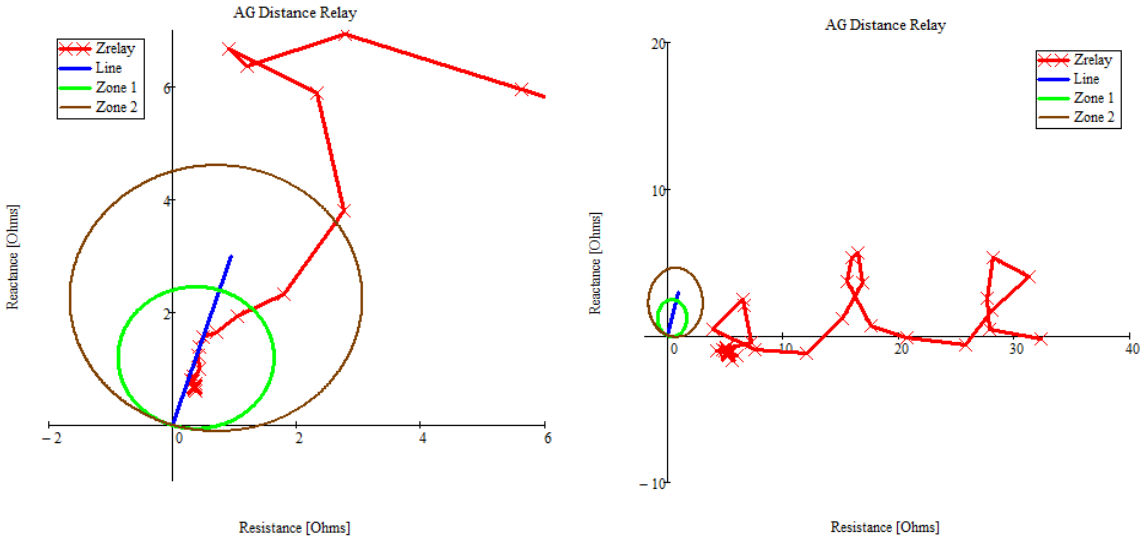

Figure 4.9. DER1 Distance Relay with Thevenin Source (left) and Norton Source (right)

On the left-hand plot in Figure 4.9, for a Thevenin source, the starting impedance location has been cropped at the right-hand edge, but after the fault it moves close to the blue line, and well within Zone 1. One might expect the post-fault impedance to settle near 0.86 + j 2.18 Ohms, which is the positive-

sequence impedance of the 3500 ft of line directly between DER1 and the fault location. The observed fault impedance is less than half that value, due to the effects of tapped loads.

On the right-hand plot, for a Norton source, the starting impedance is resistive, with a value of about 32 Ω. During the fault, this impedance migrates toward the origin, and settles at a value of about 4 Ω, primarily resistive. This value does not lie within either Zone 1 or Zone 2, so a distance relay set to cover the line between DER1 and the substation would not trip.

Memory-based incremental quantities (Schweitzer and Kasztenny2017; Blumschein et al. 2014) can produce a useful operating quantity for both Thevenin and Norton DERs; see Equations (1) and (2).

$$V_{ref} = V_a - \left|Z_{HSD}\right| I_a \tag{1}$$

$$V_{op} = -V_{a\Delta} + \left|Z_{HSD}\right| I_{a\Delta} \tag{2}$$

Figure 4.10 shows the Phase A voltage and current waveforms for an SLGF occurring at 10 cycles, under conditions similar to those in the right-hand panel of Figure 4.9. Compared to the line-to-line fault waveforms in the right-hand panel of Figure 3.3, there is very little initial phase shift in the current. In Figure 4.11, delta signals are created from differences between the instantaneous voltage and current values and their instantaneous values one cycle earlier. The first few cycles of delta signal are nonzero while a digital filter initializes, but then they settle to near zero values in a steady state, as expected. After the fault occurs at 10 cycles, both voltage and current waveforms deviate from their prefault values, and this creates nonzero delta signals. Figure 4.12 shows the operating (V_{op}) and restraint (V_{ref}) quantities from Equations (1) and (2). There are two cycles of operating quantity exceeding the restraint quantity, so a trip decision could be made quickly. However, the delta signals return to zero in a post-fault steady state, so a backup method of protection is essential.

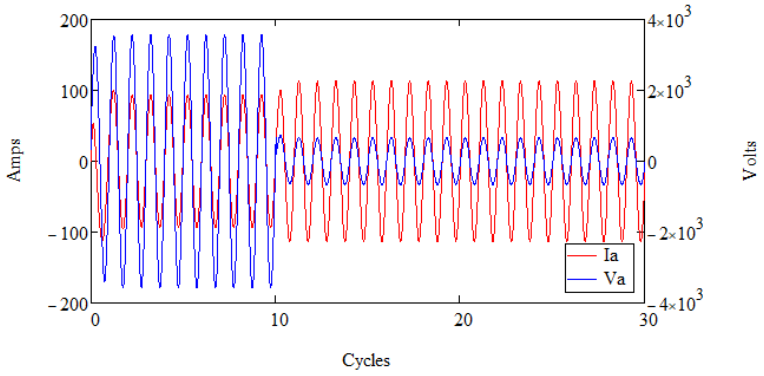

Figure 4.10. Distance Relay Voltage and Current Response to SLGF with Norton DER

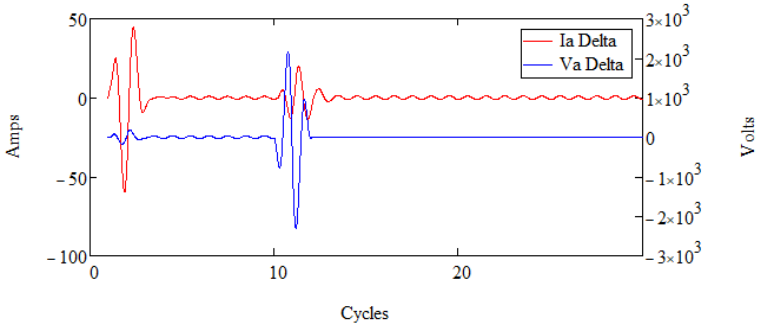

Figure 4.11. Incremental Distance Delta Quantities During Initialization and SLGF

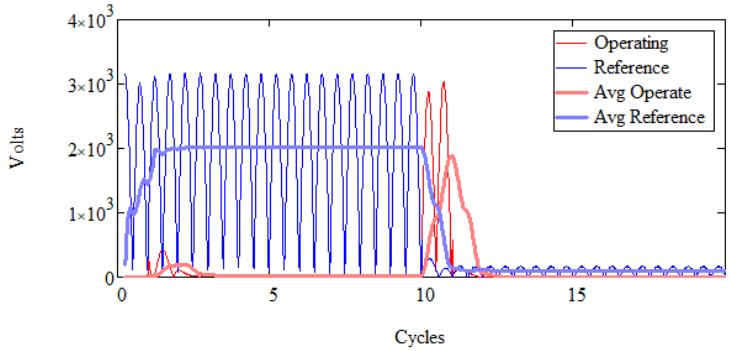

Figure 4.12. Incremental Distance Relay Operating and Restraint Quantities

4.3 Conclusion

A pure distance relay would not operate with Norton DER sources, as expected. Relays based on voltage change could operate, but will have difficulty distinguishing between must-trip and must-ride-through events. When the scheme does operate, it can trip within a few cycles.

To extend this analysis in future work,

1. Modify the MathCAD relay models to explicitly account for the source characteristics, so that expected vs. measured voltage changes can be compared for must-trip faults, to improve selectivity.
2. Consider the use of negative-sequence and zero-sequence voltage changes or impedances, to improve selectivity.
3. Perform scripted analysis of more fault types, fault resistance values, DER sizes and locations, single-phase and two-phase fault locations, and underground vs. overhead systems.

5.0 Focused Directional Relaying for Radial Distribution

5.1 Principle of Operation

Directional overcurrent relaying (Device 67) refers to relaying that determines the direction to a fault by comparing the phase angle relationship of phase currents to phase voltages (Horak 2006). The relay trips when the angle between the operating current and the polarizing voltage enters the trip zone. As with distance relays, a directional relay can use phase, ground, positive-sequence, and zero-sequence operating quantities to distinguish among the types of fault.

A 360-degree setting range is used to represent the settings of angle difference between the operating current phasor at maximum relay torque, I_A, with respect to the polarizing voltage, V_A, as shown in Figure 5.1. Because the angles between the operating current and polarizing voltage are different for normal operation and fault conditions, the 360-degree plane could be separated into several operating or nonoperating areas by setting proper limits for the minimum and maximum forward and reverse angle (Benitez et al. 2017). In Figure 5.1, the **Forward Operate Area** defines a focused trip zone, compared to simpler directional relays that use 180-degree trip zones, covering a half plane.

When a fault occurs, the phase angle between the fault current and the voltage is usually within −60 to −90 degrees (i.e., lagging) because the line, transformer, and Thevenin-source impedances are inductive. If a fault is "behind" the relay, the polarity of the current sensed by the CT will reverse, and the angle range will become +90 to +120 degrees. Both cases are different from normal load or overload conditions, when the angle ranges from −30 to +30 degrees when the power factor is 0.85 or higher, either leading or lagging. The changes in current phase angle between fault and normal conditions can be used to determine the presence and direction (forward or reverse) of a fault.

Taking Figure 5.1 as an example, for a line impedance angle of 75 degrees, the focused directional relay has an operating range of [−100, −50] degrees in a forward direction. If the system is operating normally or overloaded, the angle difference between current and voltage should be small. The angle should also be small for DER inverters operating in either forward or reverse direction. Figure 5.1 shows an example inverter operating region from −25.8 to +25.8 degrees when the power factor is 0.9 or higher. This makes it possible to distinguish overloads from faults, even with little fault current supplied from the DER.

Thus, this method is promising for distribution systems with DERs. The relay characteristic angle on distribution systems would be less than 75 degrees, because distribution lines have a lower X/R ratio than transmission systems. It may be difficult to provide a margin between the Forward Operate Area and the Normal Inverter Operating Region of Figure 5.1 when the line impedance angle is about 50 degrees. There may also be temporary overlaps during system dynamics; for example, reactive power support during ride-through events, as provided for in IEEE 1547 (2011). With adequate margin, either in angle or through time delays, this relay is expected to be more secure and selective than overcurrent relays. The focused directional relay function is widely available from several vendors. No communications are needed. It does require both VT and CT sensors, as do the distance relays.

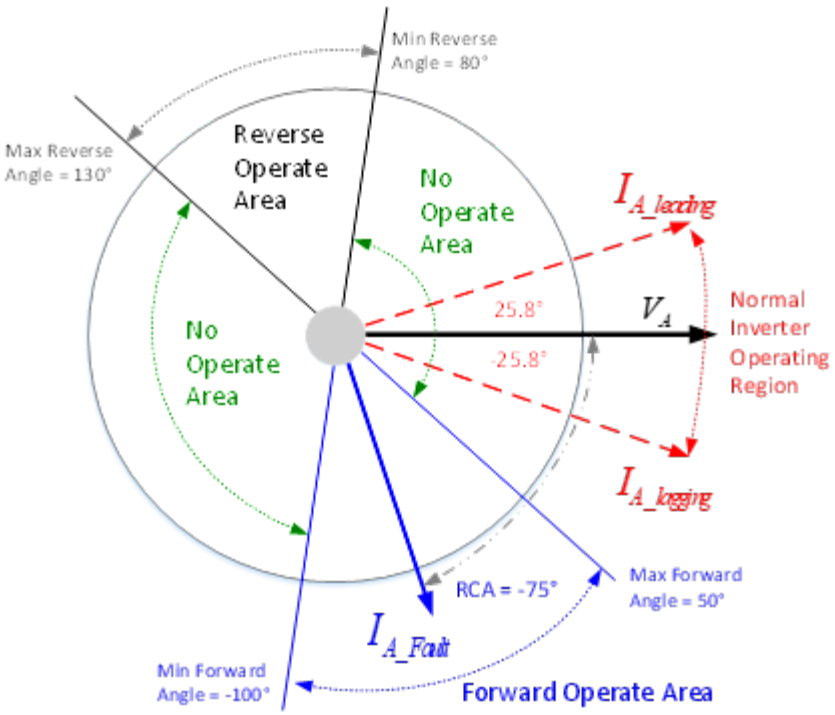

Figure 5.1. Directional Relay Zones of Operation

5.2 Analysis

The same SLGF, DER locations, and source configurations used in Section 4.0 were reanalyzed here for the focused directional relay. See Figure 3.1 for the ATP model and Figure 4.1 through Figure 4.8 for the voltage and current responses. While distance relays operate primarily based on magnitude, supervised by angle, a focused directional relay operates primarily based on angle, supervised by magnitude. Figure 5.2 shows the current angle and impedance magnitude responses at the feeder breaker, with Thevenin (rotating machine) and Norton (inverter) DERs. Each figure includes the Phase A current angle with respect to voltage, plotted in red against the left-hand vertical axis in degrees, along with the Phase A impedance magnitude, plotted in blue against the right-hand vertical axis in ohms. The current angle starts at about −37 degrees, for a load power factor of 0.8 lagging. During the fault, the current angle shifts to about −65 degrees, which is close to the line impedance angle from substation to fault. It is not equal to the line impedance angle, because loads and DER are still partially served during the fault. At the same time, a reduction in the impedance magnitude, or increase in current, indicates that a fault has occurred. For this case, overcurrent, distance, and focused directional relays at the substation would all work.

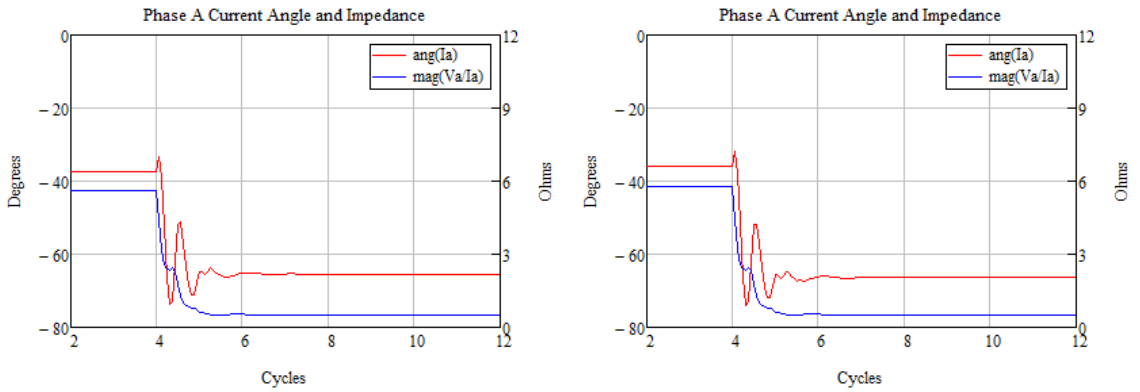

Figure 5.2. Substation Directional Elements with Thevenin DER (left) and Norton DER (right)

Figure 5.3 shows the directional response at DER1 for an SLGF, with either Thevenin or Norton DER source characteristics. In both cases, the prefault current angle is near zero degrees, because the DER injects power near unity power factor. During the fault with Thevenin DER source characteristics, the current angle shifts close to −60 degrees. This maps well into the Forward Operate Area of Figure 5.1. However, with Norton DER source characteristics, after some transients, the current angle settles to a value close to zero degrees. This lies in the Normal Inverter Operating Region of Figure 5.1, so the focused directional relay would not operate. We also tested the inverters modeled as high-impedance Thevenin sources, similar to rotating machines. By setting the impedance to 0.9 per unit, the post-fault current magnitude approximates that of a real inverter, but the current angle settles to −60 degrees with respect to the voltage. This could make the focused directional scheme appear to work with inverters, but it is not realistic.

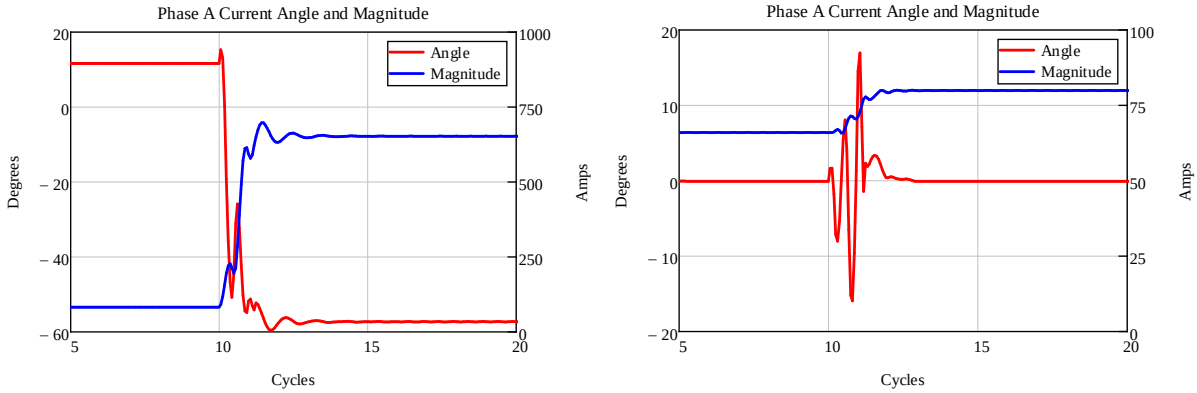

Figure 5.3. Focused Directional Currents with Thevenin (left) and Norton (right) DERs

This analysis of focused directional relaying is based on the inverter behavior. Certain types of interconnection transformer, if they present a ground source to the feeder primary, would modify this behavior for ground faults (only) (Arritt and Dugan 2008). A ground-focused directional relay may be considered for use with inverters, to operate on the ground or zero-sequence current. However, a ground relay would not be expected to operate for line-to-line or three-phase faults, so we did not analyze it further.

5.3 Conclusion

The focused directional relay works for conventional rotating machines, but not for the ideal-inverter Norton-source models considered here. It is assumed that the inverter control will act quickly to maintain the current angle close to the prefault condition, which defeats the angle change that a focused directional scheme relies on. Time delay in the inverter response might compensate for this. For example, angle tracking might be delayed for two or three cycles, giving the relay time to operate. Implementation might involve retaining a memory of the inverter current and voltage waveforms, because the inverter's PLL normally responds very quickly.

To extend this analysis in future work,

1. Modify the ATP Norton source models to incorporate angle control functions.
2. Perform scripted analysis of more fault types, fault resistance values, DER sizes and locations, single-phase and two-phase fault locations, and underground vs. overhead systems.

6.0 Single-Point Traveling Wave for Radial Distribution

6.1 Principle of Operation

Schweitzer et al. (2014) describe the basics of single-point and double-point traveling-wave protection for transmission lines. Figure 6.1 defines the main parameters of the scheme used in this analysis. When a fault occurs, the voltage suddenly drops toward zero, and the current suddenly increases. These voltage and current waves travel outward to other parts of the system, which do not "know" that a fault has occurred, nor what the ultimate fault current magnitude will be, until the traveling-wave propagations have settled to a new steady-state condition. Each time the waves encounter a circuit branch, load, or generator, there are reflections and transmissions (i.e., refractions) that alter the wave characteristics.

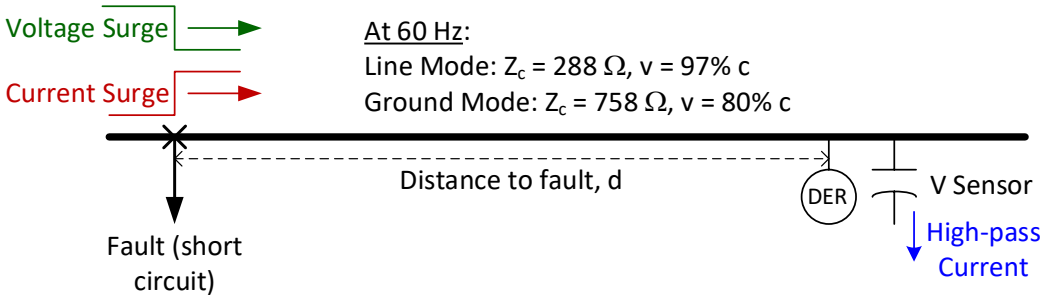

Figure 6.1. Parameters of the Single-Point Traveling-Wave Method. Z_c is characteristic impedance, v is wave velocity, and c is the speed of light in the material.

A traveling-wave protection scheme identifies the fault by signatures in the arriving current and/or voltage waves. It estimates the fault location by differences in arrival times of various traveling waves. Conventional relays operate on signals that are measured over a time frame of cycles or seconds. Traveling-wave relays operate on signals that are measured over a time frame of microseconds. Hence, the sensors and processing logic must be faster in traveling-wave relays.

As indicated in Figure 6.1, the waves travel at speeds approaching the speed of light in vacuum, c, which is 300 m/μs, or approximately 1000 ft/μs. There is an equivalence between distance, d, and wave travel time, τ, in which $\tau = d/v$, where v is the wave velocity in the same units of length (per time) as d. For example, it takes about 5 μs for a wave to travel down 5000 ft of overhead distribution line.

On three-phase lines, there are three modes of traveling-wave propagation. In the constant-parameter approximation (e.g., the "KC Lee" model in ATP), each mode has a different velocity. For overhead lines, two of these are line modes with velocity close to the speed of light, and characteristic impedance (Z_c), in the range of 250–400 Ohms. These are analogous to the line's positive-sequence and negative-sequence impedances. Z_c is the instantaneous ratio between traveling voltage and current wave magnitudes, and it is primarily resistive. An overhead line also has a ground mode, corresponding to the zero sequence, with Z_c significantly higher than the line modes, and with v significantly lower than the line modes.

Schweitzer et al. (2014) advised against using the ground mode for double-ended schemes, because of its higher distortion and attenuation compared to the line mode. In contrast, this analysis considers the difference in arrival times between the line and ground-mode waves in a single-ended scheme, also suggested in Schweitzer et al. (2014). On transmission lines, it is valid to assume there are no taps within the protected line that would desensitize traveling-wave relays. On distribution lines, there will be many such taps that distort the waves. This distortion will complicate signature identification, and also the

decomposition of waves into arriving, reflecting, and refracting components (Schweitzer et al. 2014). The shorter line lengths on distribution systems than on transmission systems mitigate this somewhat. The farther the wave travels, the more it attenuates and distorts.

Table 6.1 summarizes the sequence impedance and traveling-wave parameters for the line construction types used in the IEEE 13-bus test circuit. These are based on the line's physical spacing and conductor characteristics, which produce resistance, inductance, and capacitance parameter matrices for the line at 60 Hz (Kersting 2001). These are converted to constant traveling-wave parameters according to Equation (3), applied separately for positive and zero sequence:

$$Z_c = \sqrt{L'/C'} \qquad v = 1/\sqrt{L'C'} \tag{3}$$

Where L' and C' are the positive-sequence or zero-sequence inductance and capacitance, respectively, per unit length. For example, L' in henrys per mile and C′ in farads per mile would yield Z_c in ohms and v in miles per second. In Table 6.1, the v values are normalized to percentage of the speed of light. The line capacitance values are often ignored in distribution power flow calculations, but they are essential for determining the traveling-wave parameters.

Given Z_c and v, we can determine L' and C' using Equation (4), applied separately for positive and zero sequence:

$$L' = Z_c/v \qquad C' = 1/Z_c v \tag{4}$$

Where L' and C' will be in henrys and farads, respectively, per unit length, consistent with the units of v. If given as a percentage of c, then v should be converted to some physical unit of length per second. Equation (4) can be helpful in estimating C' when that value is not available, because L' is usually available, and reasonable defaults may be estimated for Z_c and v based on the type of line.

Table 6.1. Line Characteristics of the IEEE 13-Bus System

Code	Type	R_1	X_1	R_0	X_0	Z_1	V_1	Z_0	V_0
	Units	(Ω/mi)	(Ω/mi)	(Ω/mi)	(Ω/mi)	(Ω)	(%c)	(Ω)	(%c)
601	3ph overhead 556 ACSR	0.188	0.600	0.660	1.908	288	97.15	758	80.37
602	3ph overhead 4/0 ACSR	0.592	0.762	1.065	2.071	342	90.70	809	79.02
603	2ph overhead 1/0 ACSR	1.120	0.893	1.746	2.285	400	90.52	889	78.70
605	1ph overhead 1/0 ACSR			1.332	1.353			547	81.78
606	3ph CN cable	0.489	0.412	1.407	0.451	53.4	26.20	55.8	25.05
607	1ph tape shield cable			1.386	1.390			122	17.73

ACSR = aluminum cable, steel reinforced
CN = concentric neutral
R_0 = zero-sequence resistance
R_1 = positive-sequence resistance
v_0 = zero-sequence wave velocity
v_1 = positive-sequence wave velocity
X_0 = zero-sequence reactance
X_1 = positive-sequence reactance
Z_0 = zero-sequence characteristic impedance
Z_1 = positive-sequence characteristic impedance

Upon review of Table 6.1, there appears to be a usable difference between v_1 and v_0 for the three-phase and two-phase overhead lines. For single-phase lines, there is only one traveling-wave mode. For the three-phase CN cable, the v_1 and v_0 values are nearly equal, as are the Z_1 and Z_0 values. The CN construction is such that the phases are essentially independent of each other for ground-mode coupling, each phase having its own neutral formed by the concentric wires.

6.2 Analysis

This section is based on a single DER at the end of the line in Figure 3.2. Over the time frame of interest, it makes little difference whether the DER is a Thevenin or Norton source, which is one reason to explore this method of fault location. First, we consider the case with no transformer serving load at Bus 671, no line or capacitor at Bus 675, and very short lines from Bus 632 to Bus 633 and Bus 650. This is a more favorable situation for traveling-wave detection, with 5050 feet between the DER and the fault location, and the inductive substation impedance connected close to the fault. Second, we consider the case with everything included in Figure 3.2 and all of the lines at normal length. This is a more difficult situation for traveling-wave detection, with 5500 feet between the DER and the fault location, but with several branches and taps that will complicate the traveling-wave signatures arriving at the DER.

Figure 6.2 shows the DER currents, for a fault initiated at time 0+ of the simulation. The faulted phase current begins to change at approximately 5 μs, when the traveling wave first arrives from the fault location. Even though phases B and C are not faulted, there are coupled current waves on both of those phases, of equal and opposite polarity to Phase A. However, the changes in current take 1 or 2 μs to occur with each traveling-wave arrival. As shown in Figure 6.3, the changes in voltage at the DER are more abrupt than the current changes, so they could be easier to detect and more precisely defined for timing.

Figure 6.4 shows the currents measured in the small capacitance connected at the PCC in Figure 3.2. At power frequency, this capacitor current is negligible because the impedance is high, but the capacitance decreases in inverse proportion to frequency. A steep-fronted arriving voltage wave has high-frequency content that produces high-frequency current signals, shown in Figure 6.4. These can be detected with sensors at low voltage, while those in Figure 6.3 require sensors at high voltage.

In Figure 6.5, the power-invariant Clarke transformation has been applied to separate the individual phase signals into alpha and zero components, which correspond to a line mode and the ground mode, respectively. The Clarke transformation is an alternative to symmetrical components, and is often used for real-time applications because it does not require the use of complex numbers. Equation (5) defines the voltage transform:

$$\begin{bmatrix} V_\alpha \\ V_\beta \\ V_0 \end{bmatrix} = \begin{bmatrix} \sqrt{2/3} & -\sqrt{1/6} & -\sqrt{1/6} \\ 0 & \sqrt{1/2} & -\sqrt{1/2} \\ \sqrt{1/3} & \sqrt{1/3} & \sqrt{1/3} \end{bmatrix} \begin{bmatrix} V_a \\ V_b \\ V_c \end{bmatrix} \tag{5}$$

This decomposition clearly shows the different first-arrival times for alpha (blue in Figure 6.5) and zero (green) mode waves at 5.3 μs and 6.4 μs, respectively. Using the data from Table 6.1, with $\Delta\tau$ = 1.1 μs, we estimate 5040 ft from DER to the fault using Equation (6). This is very close to the actual distance of 5050 ft to the fault location.

$$d = \Delta\tau / (1/v_0 - 1/v_1) = 0.8673\Delta\tau \quad \text{[miles, } \mu\text{s]} \tag{6}$$

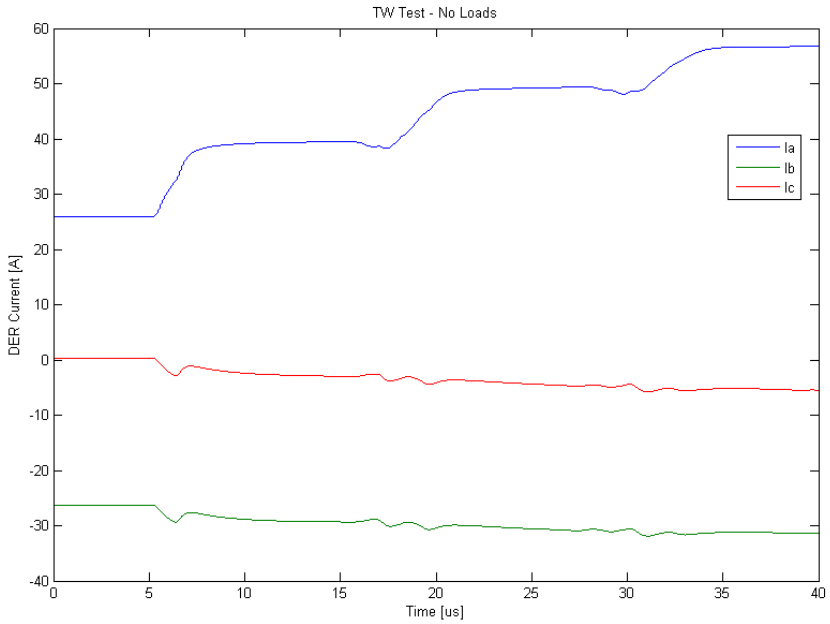

Figure 6.2. DER Currents for Single-Point Traveling-Wave Method; No Loads

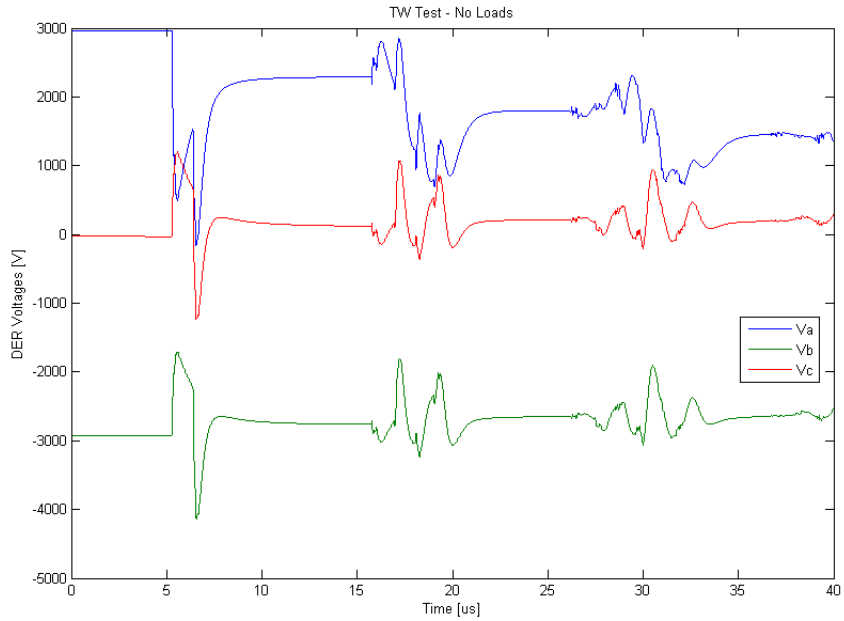

Figure 6.3. PCC Voltages for Single-Point Traveling-Wave Method; No Loads

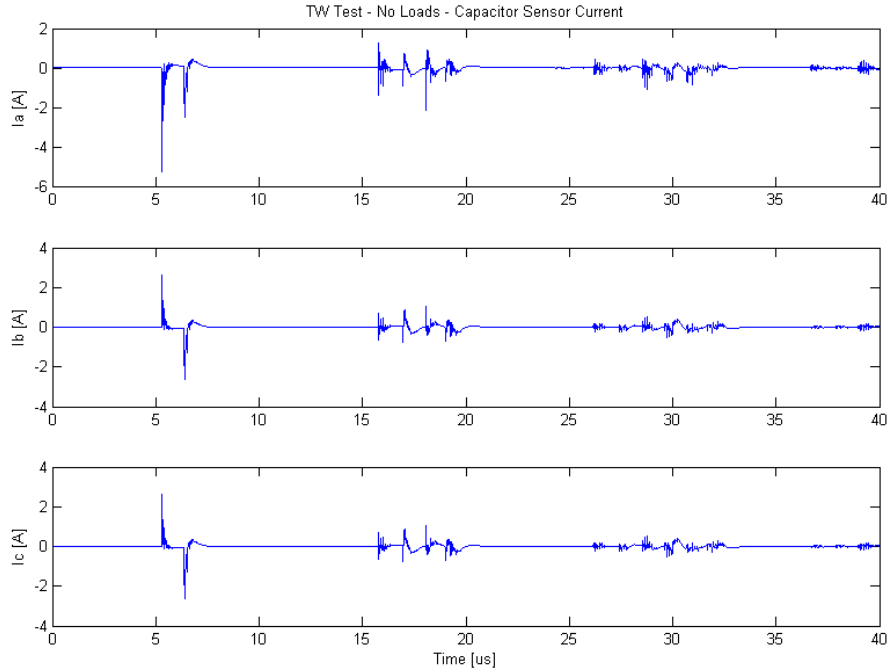

Figure 6.4. Capacitor Sensor Currents for Single-Point Traveling-Wave Method; No Loads

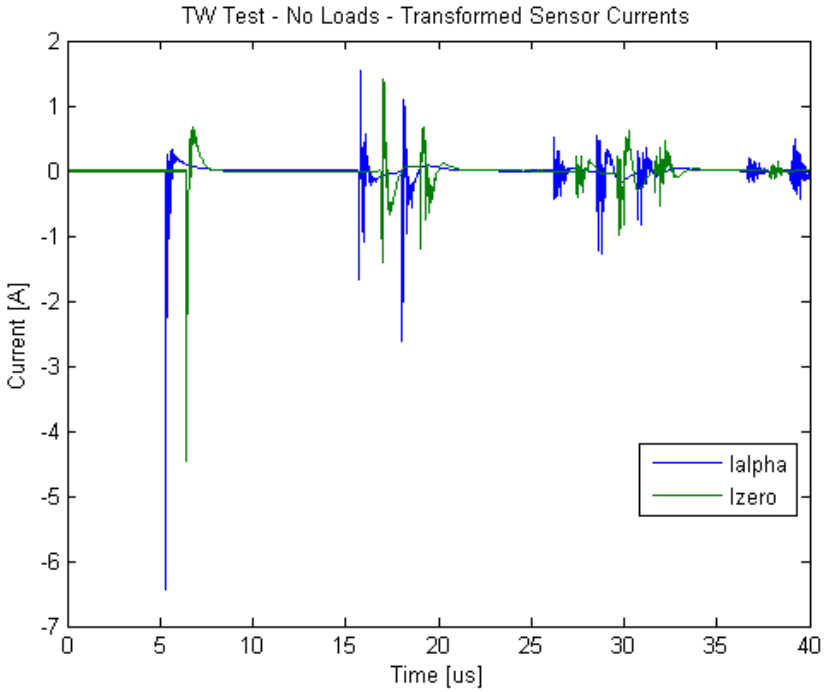

Figure 6.5. Alpha/Zero Sensor Currents for Single-Point Traveling-Wave Method; No Loads

The constant-parameter model is helpful for conceptual analysis, but frequency-dependent line modeling is important for simulating realistic waveforms. There are several formulations for overhead distribution lines, and we chose J. Marti's model for this paper (Marti 1982). A frequency-dependent model is always based on physical conductor and spacing data, and the values in Table 6.1 would then vary with frequency. Ideally, both alpha and zero modes arrive at the same time because they both travel at nearly the speed of light. They do not reach peak at the same time because of the frequency-dependent differences in attenuation and distortion. The resulting simulated ground mode will have a delayed peak compared to the line modes, which can be interpreted as a slower velocity. This makes it possible to apply the single-end method to these frequency-dependent waveforms.

As shown in Figure 6.6, the decomposition of frequency-dependent waveforms produces different apparent arrival times for alpha (blue) and zero (green) mode waves, measured as time delays between peaks. In Figure 6.6 both peaks are indicated with red brush marks, and the time difference between them is 7.78 μs. Using the data from Table 6.1, we estimate 6.75 miles from the DER to the fault using Equation (6) for line code 601.

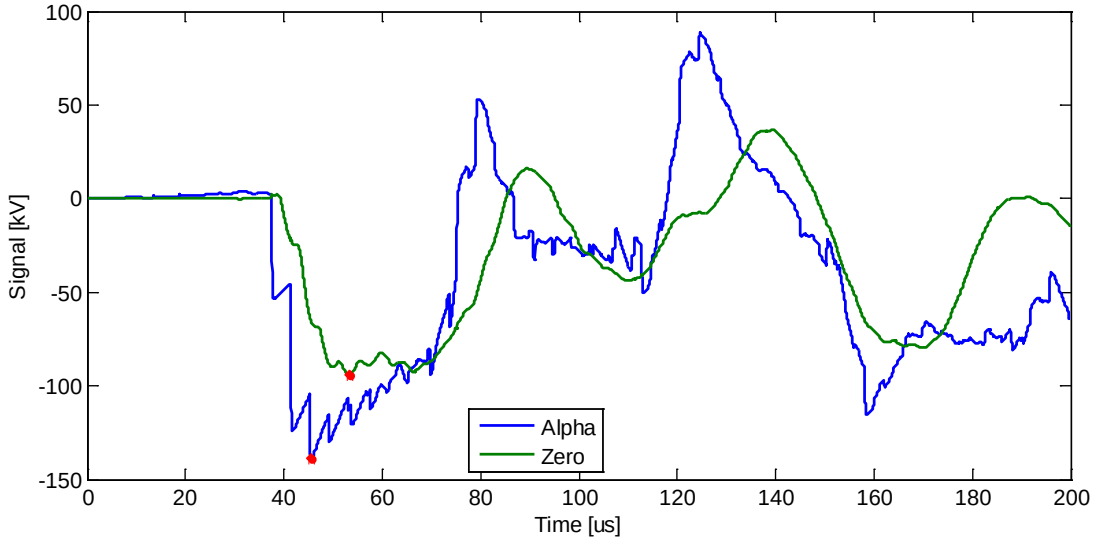

Figure 6.6. Alpha (blue) and Zero (green) Component Signals for an SLGF Seven Miles Away. The peaks marked in red occur 7.78 μs apart.

This estimate can be improved with weighted values for v_0 and v_1, reflecting changes in line construction between the DER and the fault location, but the distance error is only 3.6%.

We considered other common events on the distribution system, including load switching and capacitor bank switching, which also produce traveling-wave disturbances. The result for the capacitor switching case is provided in Figure 6.7. The distance from the DER to the capacitor bank was estimated at 1.509 miles using a difference, $\Delta\tau$, of 1.67 μs between the alpha and zero mode signal peaks. This is close to the actual distance of 1.5 miles.

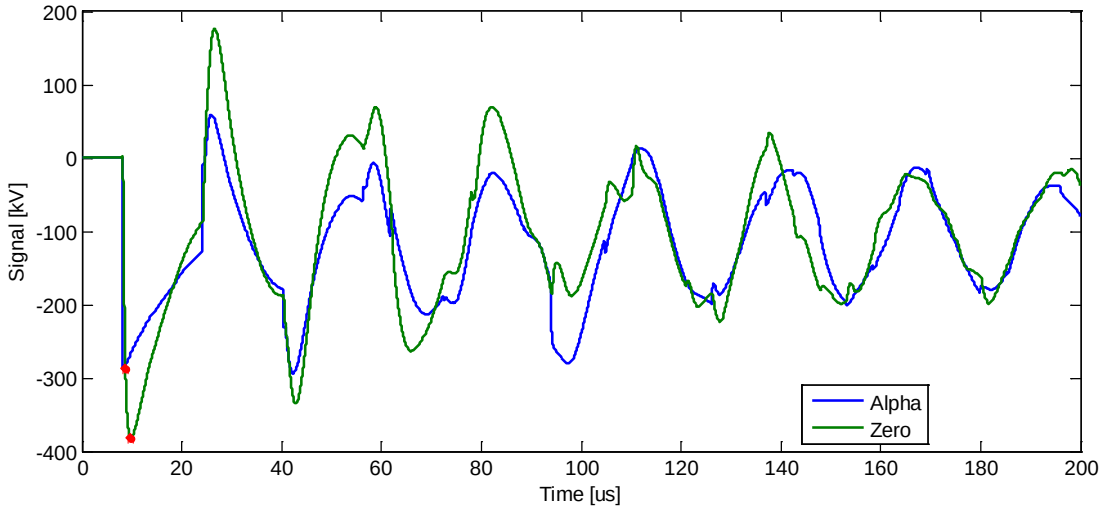

Figure 6.7. Alpha and Zero Component Signals for Capacitor Bank Switching 1.5 Miles Away. The peaks marked in **red** occur 1.67 μs apart.

6.3 Conclusion

The single-point traveling-wave method shows promise, particularly because, unlike the distance and directional schemes, it seems agnostic to whether a DER source is Thevenin or Norton type. Most faults and switching operations (even "closing into chains") will begin on a single phase, and if the event stays single phase for some tens of microseconds, the generated traveling waves should have separable alpha and zero components during that period. This is long enough to operate the relay, but a different backup scheme would be needed.

There are several open points to investigate before planning field trials of a single-point traveling-wave method on radial distribution feeders. These are planned for future work:

- Add dozens of branches and hundreds of load-serving transformers to the model structure in Figure 3.2. This would be typical of a real feeder, and is expected to limit the method's sensitivity.
- Catalog the expected signatures for all fault types. These have to be differentiated from other events, like load switching, capacitor switching, and tap changes, which also produce traveling waves.
- Explore alternative traveling-wave-based methods for three-phase cables and single-phase lines, which might not have readily separable alpha and zero modes.
- Perform scripted analysis of more fault types, fault resistance values, DER sizes and locations, single-phase and two-phase fault locations, and underground vs. overhead systems to apply the metrics in Table 2.1.

The requirement of using a capacitive voltage sensor is also a cost issue. Digital filtering on the PCC voltage might provide an equivalent signal, but only if the PCC voltage sensor has adequate frequency response and the digital filter operates fast enough. The relay must be able to resolve time differences of 0.1 μs to 1.0 μs.

The relay must detect and operate on the first wave arrival. After that, wave reflections and refractions from other components in the system would probably make the relay insecure from false operations. This

means that a traveling-wave relay could fill the same role as instantaneous overcurrent relays, which trip immediately when the current is so high that the fault location is certainly nearby. A slower-acting function would have to be provided complementary to the traveling-wave function, as time-overcurrent relays are comparable to instantaneous overcurrent relays. The single-ended, traveling-current-wave method suggested recently in Guzmán et al. (2018) could mitigate the need to operate on the first wave arrival. However, the multiple taps and loads on distribution systems could still make this difficult.

7.0 Smart Network Protector Relay for Secondary Networks

No reverse power flow can be allowed through the NWP during normal operation. Existing practice is to limit DERs so that reverse power flow is prevented, whether at the building, facility, or network level (Anderson et al. 2009, Bokhari et al. 2016, Mohammadi and Mehraeen 2017, IEEE 2011). This would preclude high penetration of DERs on secondary networks. To allow more DERs, some measures without significant changes of device/system configurations can be implemented:

- Set the network relays to be less sensitive to reverse power flow (for example, by adding a time-delay mode).
- Set the relays not to trip for low-level reverse power flow at all.

However, they are only short-term solutions, which may work for low-level reverse power flow cases but not for the systems where DER penetration is high and large bidirectional power flow is a part of normal operation.

7.1 Principle of Operation

A cut-set scheme has been proposed for protection of secondary networks with DER. The idea is to define a virtual enclosed boundary (called a "cut set") and check the net current flowing into the boundary to determine whether the network protector(s) should be tripped (Mohammadi and Mehraeen 2017). The boundary will cross all the feeders, and include all the network protectors, but exclude any loads, as depicted in Figure 7.1. The cut set functions like an extended differential scheme, incorporating lines, transformers, and switchgear.

The currents at the places where the defined boundary is intersecting the feeder and network lines will be measured and sent to the NWP relay for analysis. The relay will use the signed summation of all these current measurements to determine whether the reverse power flow is generated by a feeder fault inside the boundary or by the normal operation of DERs, and operate (trip or not) the circuit breaker accordingly. To implement the approach, the sensitive mode of a network protector relay should be adjusted so that the network protector will be tripped only when the reverse power flow is detected and the net current is nonzero.

For one system, there may be more than one way to define the virtual boundary. Two possible definitions of the virtual boundary are shown in Figure 7.1. Different virtual boundaries have different protection coverage areas. This scheme will only be effective in the feeder and network sections enclosed inside boundary. The larger boundary covers a larger area, but usually would require more measurement and communication capabilities.

Since there are no current sources or sinks (loads) included inside the boundary, all the currents will only flow through the enclosed boundary during normal operation. By Kirchhoff's current law, the signed summation of currents into the boundary should be zero, regardless of the direction of power flow. However, any upstream feeder fault that occurs inside the boundary will cause the net current to be nonzero. If the virtual boundary is well defined, the net current into the boundary will be a good indicator of the existence of a feeder fault. By associating the net current measurement with the reverse power flow detection, the network protector relay can distinguish the real cause of the reverse power flow, (by feeder faults or excessive DER generation), and trip the protector only for faulty reverse power flow, not for normal conditions.

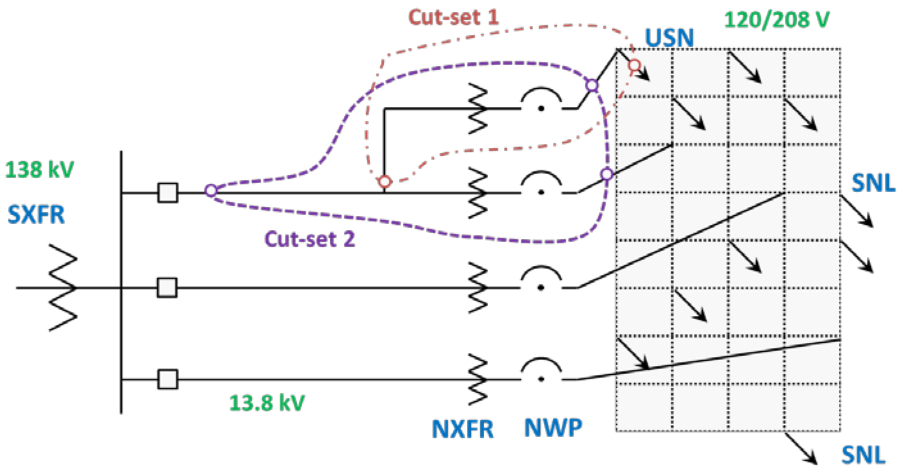

Figure 7.1. Two Examples of a Virtual Boundary ("Cut Set")

Network protectors are designed to trip when they sense reverse power flow to protect the low voltage (secondary) network against upstream feeder faults. However, DERs interconnected in secondary networks may also create reverse power flow when their generation is larger than the local load consumption. The network protector does not differentiate the reverse power flows induced by faults or normal DER operation. It prevents excessive power generated by the DERs during normal operation from back-feeding the feeders. For this reason, DERs are not allowed to back-feed the upstream feeders in most secondary network applications. In common utility practice, DER generation is monitored to maintain a minimum load for the whole network, preventing the power back-feeding. Some relays (e.g., minimum import relay, reverse power relay) may be used to trip the DER units when the minimum load requirements cannot be met (Anderson et al. 2009, Passey et al. 2011).

At its core, this proposed method is a generalized differential current protection method. It only modifies decision logic of the sensitive model of the regular network protector relay, and does not affect the protective characteristics of other modes of the relay. If the data communication and analysis (summation of the current measurements to obtain the net current) can be done in time (in six cycles [Mohammadi and Mehraeen 2017]), the speed of the relay under the sensitive model will not be affected.

The method requires current measurements at all the points where the virtual boundary intersects the feeder lines/protectors. It also needs communication infrastructure/channels for transferring the current measurements to the relays. For modern microprocessor-based network protector relays, it takes six cycles to trip under sensitive mode (Mohammadi and Mehraeen 2017). The transfer of current measurements and calculation of the net current should be completed within six cycles, if the proposed approach is to be implemented. This might not be a problem for small secondary network systems, where the number of required current measurements and geographic distances for communication are relatively small. However, the scheme may become not feasible for large systems due to high costs of measurement and communication.

In addition to the cost for regular network protection, the cost for the proposed method should also include protection for the data measurement, communication, and analysis. This may not be economically efficient for secondary networks with large and complicated system configurations. The project team found no report of implementation of the method in real systems.

7.2 Analysis

Figure 7.2 shows the low-voltage secondary network test circuit used for evaluation (Schneider 2014). The test bed has eight primary feeders feeding a 120/208 V secondary grid, plus eight 277/480 V secondary spot networks. The secondary networks are all wye grounded, and the 13.2-kV primary feeders are all delta connected. Many of the impedances are very small in this type of circuit. In a meshed network of small impedances, the fault currents are much higher than in radial circuits, e.g., <100 kA vs. 20 kA. It is not difficult to calculate the total fault current at a point, but small changes in parameters can produce large changes in the division of this fault current between parallel paths. This uncertainty has to be accounted for in coordinating relays and fuses. It can also affect the selection of secondary cable fuses (see Figure 1.13) because the division of load currents is also very sensitive to small changes in component impedance.

To perform the analysis, a cut set was created on Feeder 8 that included the following nodes: P135, P136, P138, and P141. The set includes the line to Node P143, but it does not include Node P143. Distributed generation was attached at Node P141. The cut set is illustrated in the shaded portion of Figure 7.2.

For testing purposes, DER was located outside the cut set at Node P141, and the NWP did not trip due to DER current. Faults inside the cut set always produced a strong trip signal. However, faults outside the cut set often also produced a small but nonzero signal, so that either time delays or less sensitive settings might be needed to avoid false trips. Figure 7.3 shows an example for a bolted three-phase fault at 3 s at Node P149, with point-by-point calculation of the net cut-set current waveform. In this case, the cut-set aggregate does not stay at exactly zero while the fault is present on the system. This may be due to simulation artifacts or wave form sampling. To avoid misoperation, the blocking threshold for the protection scheme would not be set to exactly zero.

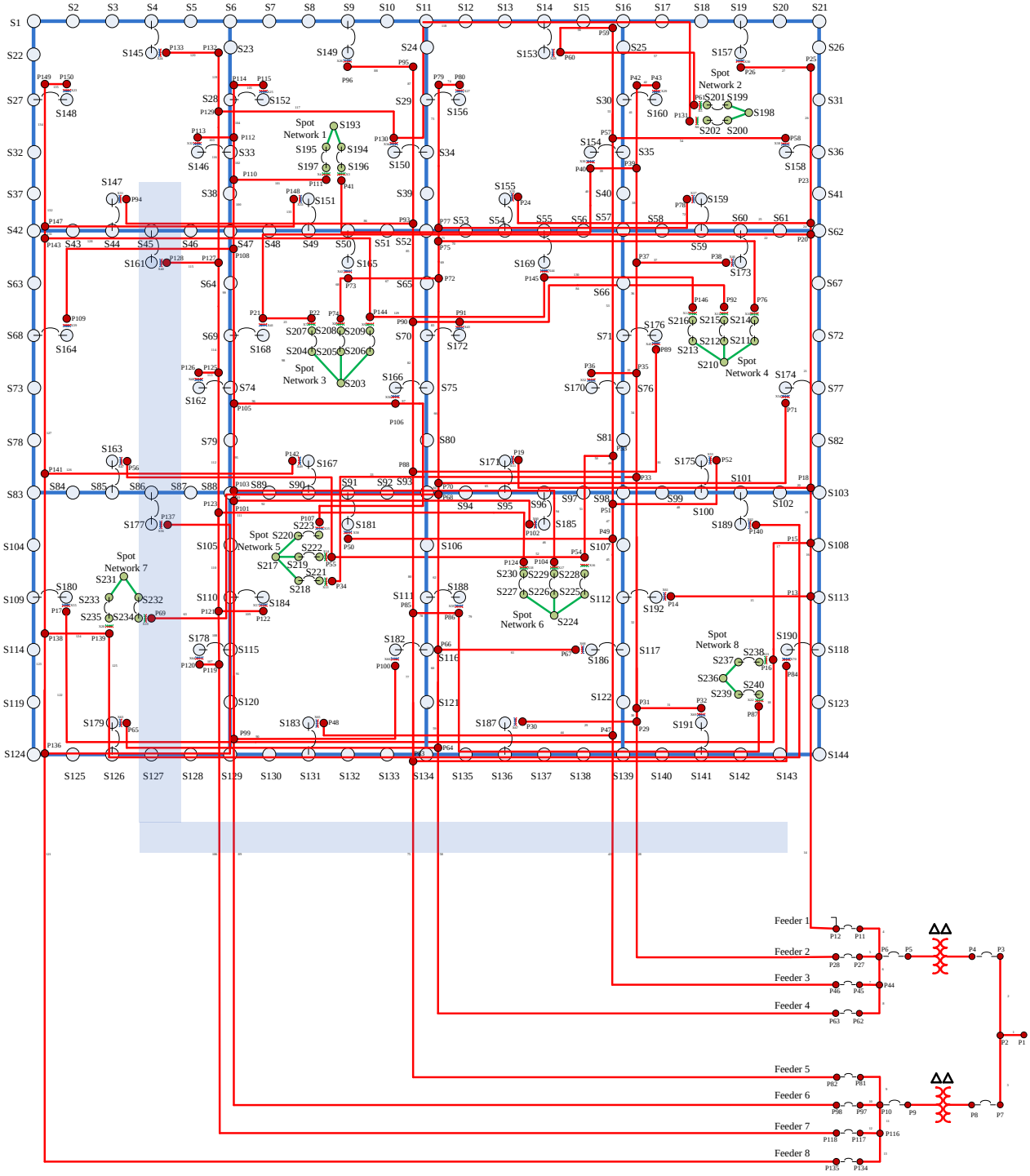

Figure 7.2. Low-Voltage Secondary Network Test System with a Cut Set

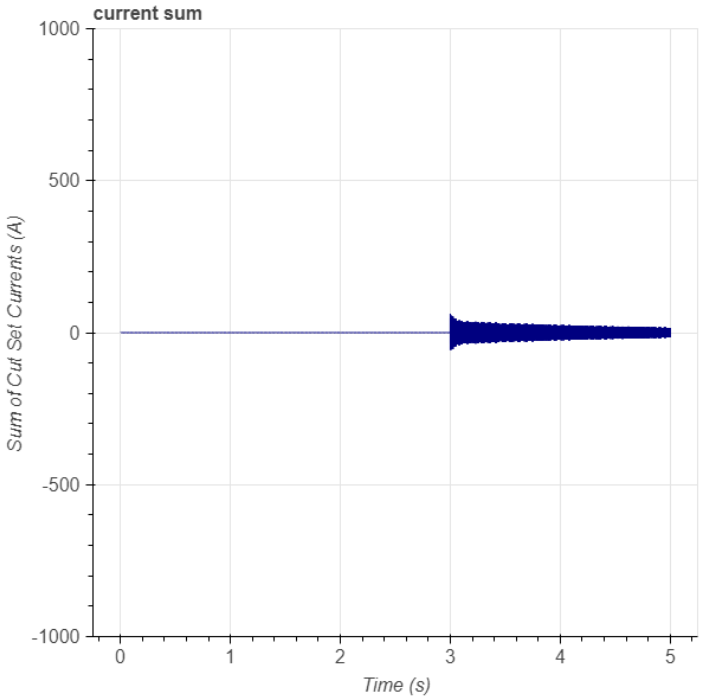

Figure 7.3. Current Aggregate, Fault Outside Cut Set

While analog differential techniques may be feasible in some cases (typically where the network covers a small geographical area), a communication-based technique using current phasors is a more likely scenario. An implementation of a phasor-based current aggregation technique is shown in Figure 7.4 for faults inside and outside of the cut set.

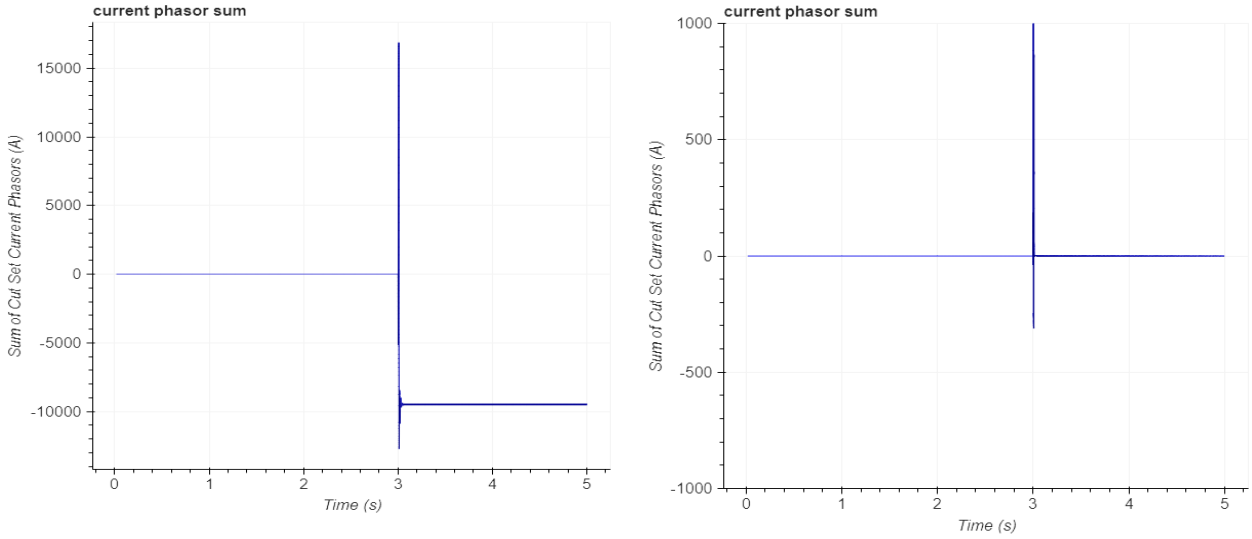

(a) Fault inside cut set

(b) Fault outside cut set

Figure 7.4. Phasor-Based Current Aggregation

As with the point-by-point aggregation method, the phasor aggregation method has no trouble differentiating between faults inside and outside of the cut set. To be useful, however, the technique must

be able to provide actionable information to the networked protector before the protector opens for reverse power (typically six cycles or around 0.1 s). Figure 7.5 shows an expanded view for the scenario where the fault is located within the cut set. In this case, the phasor aggregation method was able to detect the event and come to an approximate steady state in about one cycle (the sample window for the RMS calculation). Performance may be improved by using a smaller sample window; however, response times in this range should allow sufficient time for communication and analysis of the data before network protector operation.

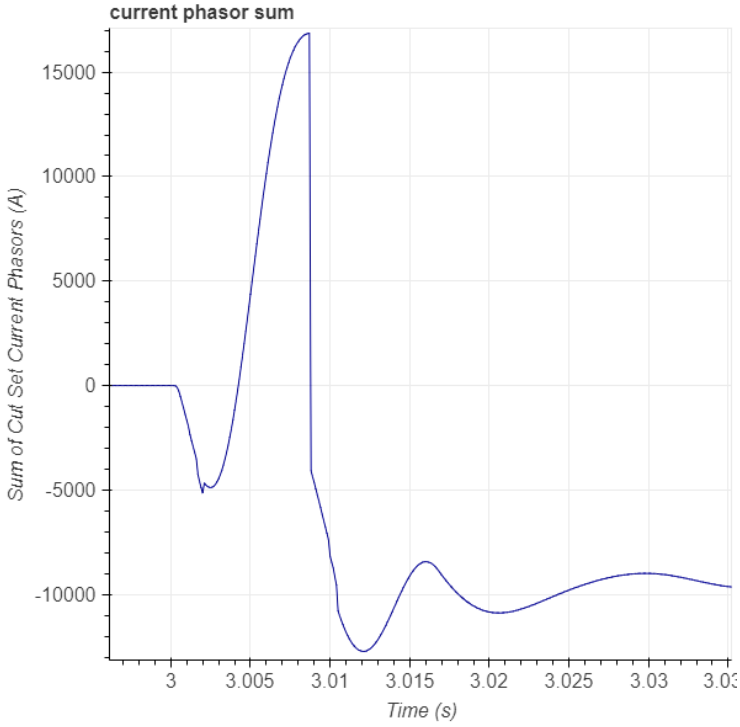

Figure 7.5. Phasor-Based Aggregation, Expanded

7.3 Conclusion

By means of ATP simulation, we found that a cut-set differential scheme could work on secondary networks, but it does require communications between the substation and each NWP. The cut set functions like an extended differential scheme, incorporating lines, transformers, and switchgear.

Distance relays were considered that look back into the primary feeder, but many NWP vaults lack space for the required submersible VT and CT sensors. Some utilities have desensitized the NWP relay trip setting in order to accommodate possible reverse power flow from DERs. The NWP still trips at current levels representative of multiphase primary feeder faults, but may not trip for the SLGF. Also, if the NWP has to open after the primary feeder opens without a fault, communications are required. Before desensitization, the NWP would have tripped in that situation based just on the reverse supply of transformer magnetizing current and circulating flows through closed NWPs. In all cases, the scheme needs to handle cases where the primary feeder also supplies "regular" load, not just secondary networks. We have not yet identified a state-of-the-art solution that meets all the objectives stated earlier.

8.0 Transform and Admittance Methods for Microgrids

8.1 Principles of Operation

Two promising alternate protection schemes are evaluated that can operate with or without fault current: the differential S-transform method (Kar and Samantaray 2014) and the admittance (or mho) method (Dewadasa et al. 2008b). As Figure 8.1 indicates, they might be applied synergistically on a microgrid, with the S-transform method used for lines and transformers, while the mho method is used for buses and loads.

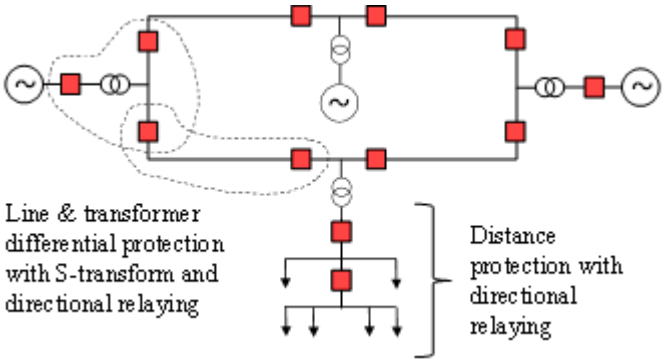

Figure 8.1. Proposed S-Transform and Admittance Schemes for Microgrids

The S-transform is a time-frequency transform that preserves phase information.[1] The discrete S-transform (DST) version is used in this study, as given in Equation (7):

$$S[j,n]=\sum_{m=0}^{N-1}X[n+m]\exp\frac{-2\pi^2m^2k^2}{\left(a+b\sqrt{|f|}\right)^2}\cdot\exp\frac{\mathbf{i}2\pi mj}{N} \tag{7}$$

where $X[n]$ is the discrete Fourier transform of the signal $x(k)$ in Equation (8):

$$X[n]=\frac{1}{N}\sum_{k=0}^{N-1}x[k]\exp\frac{-\mathbf{i}2\pi mk}{N} \tag{8}$$

In the preceding Equations (7)–(8), j = 1,2,…N − 1 is the time index, and n = 0,1,…N − 1 is the frequency index. The energy is defined in Equation (9) as

$$E[j]=\sum_{n=0}^{N-1}\left|S[j,n]\right|^2 \tag{9}$$

For protection, the difference in energy of the S-transformed sending and receiving current is used as an operating quantity for tripping. The energy difference is a quantity that is robust against communications transport delay.

[1] This is <u>not</u> the Laplace transform, which is denoted by lower-case s.

The admittance method has the following advantages over the DST method: it does not require communications, paired protection on either end of the protected element, or hardware capable of carrying out time-frequency transforms in real time. It is also suitable for protecting load buses.

8.2 Analysis

To test the two proposed microgrid schemes, the case study system of Figure 8.2 is used, with the parameters listed in Table 8.1. This consists of a two-bus microgrid operating in stand-alone mode while supplied by a grid-forming inverter at Bus 1. The inverter operates with a proportional-resonant (PR) controller, as described by Vasquez et al. (2013). The PR controller has advantages over a proportional-integral controller in that it does not require measured quantities to be converted into a rotating reference frame, which makes it more amenable to implementation on fixed-point controllers, and it also can compensate for low-order current harmonics.

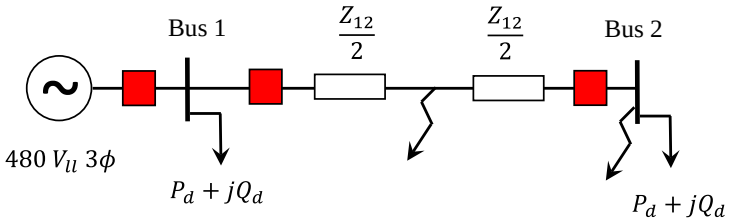

Figure 8.2. Microgrid Case Study System

Table 8.1. Microgrid Test System Parameters

Parameter	Symbol	Value
Inverter voltage	V_{ll}	480 V
Inverter frequency	f_0	60 Hz
Inverter peak current limit	I_{max}	300 A
Line resistance	$Re(Z_{12}) = R_{12}$	78 mΩ
Line Reactance	$Im(Z_{12}) = X_{12}$	53.4 mΩ
Load real power	P_d	25 kW
Load reactive power	Q_d	12.5 kvar
Fault resistance	R	0.433 Ω

The modeled inverter has two control loops: an inner current/voltage control loop that regulates the AC voltage on the output LCL[2] filter capacitor and an outer droop/virtual impedance control loop. At the time constants of interest (tens of cycles), only the inner voltage control loop is of interest, while the outer control loop responds on the order of seconds. Because the PR controller operates in a stationary reference frame, it has the disadvantage that if the current control reaches the maximum output, the current will produce output voltage harmonics, and any protection employed will need to be robust against such harmonics.

[2] LCL is a filter with two inductors and one shunt capacitor.

To test the DST for protection, a pair of simulations was carried out on the Figure 8.2 case study system with faults at the midpoint of Line 1-2 and at Bus 2. The relay is at Bus 1, looking to the right to protect Line 1-2. It should operate for a fault at the midpoint, but not for the Bus 2 fault. Figure 8.3 illustrates the decrease in inverter output voltage and the appearance of waveform distortion after 0.25 s, as the inverter goes into current-limiting mode. Figure 8.4 illustrates the sending and receiving currents on either end of Line 1-2. Figure 8.5 shows the resulting differential DST energy for both fault locations. The signal is positive for the midpoint fault (should trip) and oscillatory for the Bus 2 fault (should not trip). After averaging, this energy signal can form the basis of a relay operating quantity, by comparison to a threshold.

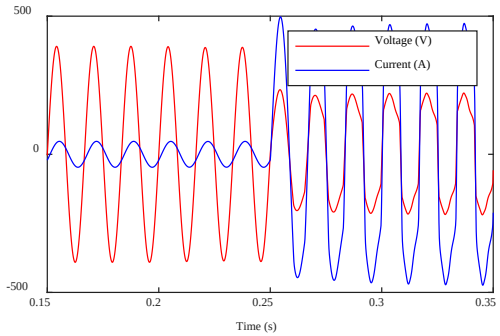

Figure 8.3. Voltage and Current for a Midpoint Fault with 1/4 Cycle Delay

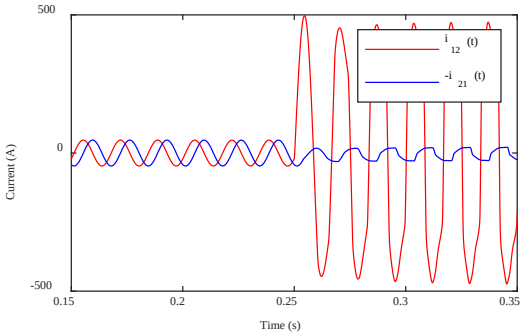

Figure 8.4. Sending and Receiving Currents for a Midpoint Line-Neutral Fault with 1/4 Cycle Delay

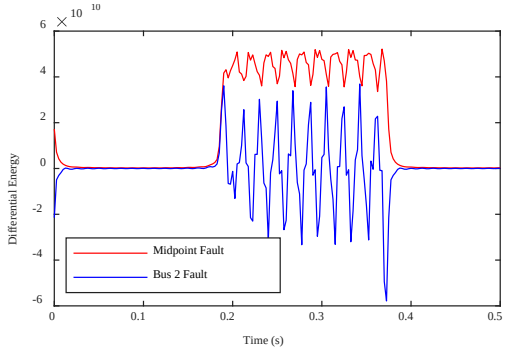

Figure 8.5. Discrete S-Transform Differential Energies for Line-Ground Faults with 1/4 Cycle Delay

A limitation of the method is that some ripple is present in the energy because of the current harmonics, so smoothing is necessary at the cost of response time. An additional issue not demonstrated here is that if

two inverters are present on either end of a line so that their fault contributions are identical, the protection will not respond. In such a case, either backup protection is required, such as negative-current, zero-current, or overcurrent relaying (Nikkhajoei and Lasseter 2006), or the method must be extended to add a signed quantity to the differential energy through directional protection. Both of these alternatives carry limitations: the first can result in false trips in the case of severe load imbalance, and the second requires the addition of voltage sensing. To test the admittance protection, the same pair of simulations was repeated with the relay at Bus 2, looking to the left to protect Bus 2. It should operate for the Bus 2 fault, but not for the midpoint fault. The results are illustrated in Figure 8.6 and Figure 8.7. Figure 8.6 shows the measured impedance dropping into the trip region, while Figure 8.7 shows the impedance dropping and then recovering. Previous work has documented that admittance protection can result in false trips for upstream line-to-ground faults (Dewadasa et al. 2008a, 2008b). Figure 8.7 indicates that this behavior occurs briefly in the case study system, and either directional protection or time-delay coordination (Dewadasa et al. 2009) is needed to overcome this.

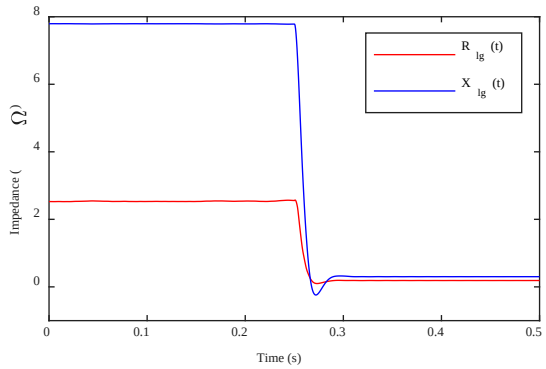

Figure 8.6. Line-Ground Impedance for a Bus 2 Line-to-Ground Fault

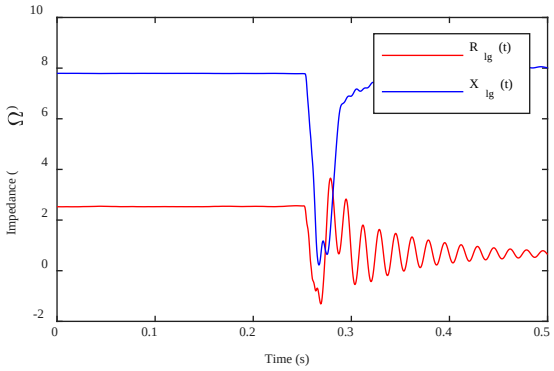

Figure 8.7. Line-to-Ground Impedance for a Midpoint Line-to-Ground Fault

8.3 Conclusion

For microgrids with fault-capable generation, directional overcurrent protection is the most cost-effective method. In the case of microgrids with inverter-interfaced distributed generation, differential protection of lines is necessary. Traveling-wave protection is unlikely to be cost-effective, because it requires high sampling rates, centralized control, and time synchronization.

Differential protection that makes use of wavelet transforms offers the potential for more robust and cost-effective protection systems, because they have more relaxed time-synchronization requirements. However, differential protection requires sensing on each end of a protected line segment, which increases cost. For this reason, if it is used, it will likely be restricted to the primary voltage portion of the microgrid and combined with an alternate scheme for the secondary portion. On the secondary portion of the microgrid at load buses, if the ratio of fault current to maximum load current is sufficient (for loads connected via a transformer that is small relative to the total power rating of the microgrid generation), then conventional time-overcurrent protection can be applied. If that is not the case, then impedance-based protection will provide the necessary sensitivity.

9.0 Ranking and Gap Analysis

This section ranks the existing protection schemes and near-term possibilities according to five of the metrics categories from Table 2.1. These rankings may be used to select candidate schemes for development and demonstration projects occurring within a year or two. Another near-term effort is described to develop inverter-based DER models that are suited for validation and widespread use.

9.1 Protection Scheme Rankings

Table 9.1 summarizes the performance of protection schemes on radial systems, after filtering out the limitations of essential event categories (i.e., selectivity, security, dependability) from Table 2.1. Only four estimated levels are used, from 1 (best) down to 4 (worst). These rankings are necessarily subjective, because exhaustive studies have not been done yet. Sensitivity refers to the ability to detect ground faults with resistance. Flexibility refers to the amount of DER that can be connected. Speed refers to the detection time. Cost includes installation, maintenance, and training for the relays, sensors, and communication systems. Maturity refers to the number of vendors and the availability of existing products to implement the scheme. Existing relay schemes are shaded. The following is for the relay schemes on radial systems:

- Sensitivity: Undervoltage trip is the least discriminatory, and traveling wave is potentially the best. Among the others, directional overcurrent is less suitable for inverter-based DER because it does not use voltage sensing.
- Flexibility: Incremental and traveling wave types are potentially agnostic to the amount and type of DER. The undervoltage trip is least flexible, and the current-based schemes are also not very accommodating for inverter-based DER.
- Speed: Traveling-wave and incremental relays are fast, but their trip signals will not be persistent. The others require time delays.
- Cost: Traveling-wave relays will require new high-frequency sensors. Directional overcurrent relays require only low-frequency CTs, while the others also require VTs. In addition, incremental relays will need some custom programming.
- Maturity: All existing schemes are well established. There is only one vendor of traveling-wave relays, and they have not been tested yet on distribution systems. Focused directional relays have been applied at industrial facilities. Incremental algorithms are not yet consistent among vendors.

Table 9.1. Ranking of Protection Schemes for Radial Feeders. (1 = best)

Scheme	Sensitivity	Flexibility	Speed	Cost	Maturity
Autoloops added to relays	2	3	4	2	1
Direct transfer trip added to relays	2	2	2	4	1
Permissive transfer trip added to relays	2	2	4	3	2
Directional overcurrent	3	3	4	1	1
Distance relays	2	3	2	2	1
Undervoltage trip	4	4	3	2	1
Conventional generator device numbers	2	3	2	2	1
Incremental quantities	2	1	1	3	3
Focused directional	2	3	2	2	2
Traveling wave	1	1	1	4	4

The first three rows in Table 9.1 refer to auxiliary components of a protection scheme, namely transfer tripping and reclosing. They are not methods that will detect a fault in the first place, but new relays would need to interoperate with these switching schemes. Autoloops and permissive transfer trip are less expensive than DTT, but they may not be fast enough for some use cases. Better communication schemes are still needed. In summary, the three proposed relay schemes in the last rows of Table 9.1 merit more evaluation. There are uncertainties with all of them; it may be the case that only one is found suitable.

Table 9.2 ranks the schemes for secondary network protection. Current practice, sometimes called de minimis (IEEE 2011), is well established, but it severely limits the quantity of DERs that can be accommodated. Two examples given in the standard limit aggregate DER to 1/15 or 1/50 of minimum load on the network (IEEE 2011). Some utilities have begun to desensitize the reverse power trip function, which helps accommodate more DERs. However, it does require communications to provide the same level of dependability and security. Cut-set differential schemes could work, but they will require high-speed communications to several points on each feeder, and sensors in hard-to-reach locations. The same applies to distance relaying, with additional uncertainties in whether a distance relay would detect all conditions for which the NWP must actually trip. Neither cut-set nor distance scheme is mature enough for a field trial yet.

Table 9.2. Ranking of Protection Schemes for Secondary Networks. (1 = best)

Scheme	Sensitivity	Flexibility	Speed	Cost	Maturity
De minimis	1	4	1	1	1
Desensitize	1	3	1	2	2
Cut sets	1	1	1	4	4
Distance	2	2	4	3	3

Table 9.3 ranks the protection schemes for microgrids. Both the signal-transform and admittance methods are promising enough to justify further simulation work and algorithm development. The admittance method would be easier to implement with existing products. The signal-transform method would involve programming a real-time computer for each installation, but deployment could be automated.

Table 9.3. Ranking of Protection Schemes for Microgrids. (1 = best)

Scheme	Sensitivity	Flexibility	Speed	Cost	Maturity
Adaptive directional	2	2	3	1	1
Discrete S-transform	1	1	1	3	3
Admittance	2	2	2	2	2

9.2 Type Testing for Inverter Models

Inverter-based DERs behave differently from conventional generators under fault conditions, voltage excursions, and frequency excursions. Throughout this report, we have illustrated the importance of fault current magnitude and angle to protection system response. For examples, see Figure 3.3 and Figure 4.9. In this study, a simple PLL model was developed to simulate a typical inverter's dynamic behavior. But this model may not represent all real inverters. To illustrate, an example from a low-voltage inverter test program appears in Figure 9.1. The fault occurs some distance away, causing the voltage to sag to 60% of normal at the microinverter terminals. The microinverter momentarily attempts to restore full power output, and then it curtails the power. This type of behavior is unexpected and would complicate protection studies.

Rotating machines also have time-dependent behaviors, which are divided into a subtransient region for breaker ratings, a transient region for protective relaying and stability, and a steady-state region for power control. The modeling and application issues were solved over a period of many decades, by developing equivalent voltage-source models for steady-state and dynamic conditions, in parallel with supporting type tests that enabled model validation and use. New synchronous generators come with a set of resistance, reactance, and time-constant parameters on data sheets that match the formats expected by commercial protection and stability software tools. Important generator control system models are also widely available (IEEE 2016).

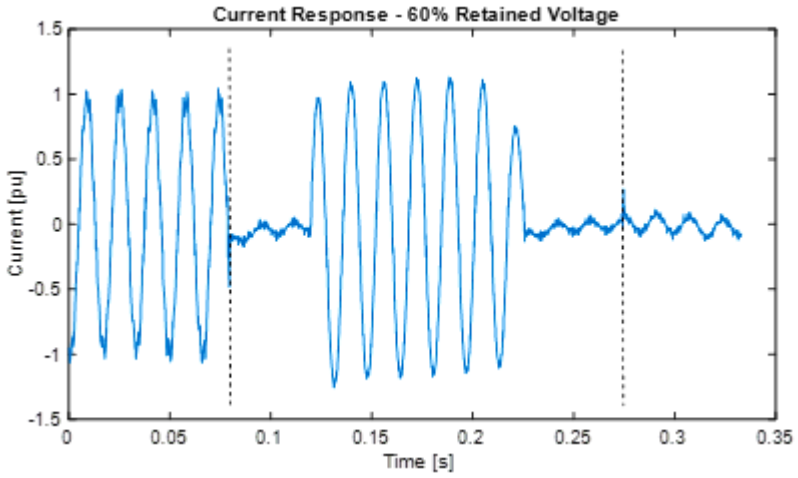

Figure 9.1. Microinverter Response to a 60% Voltage Sag

The same degree of model standardization needs to happen for modern grid equipment, but with equivalent current-source models for power electronics. Several researchers and tool vendors have worked on prototype models, but they are not supported with equipment type tests that produce the model parameters. The most accurate models are developed by the equipment vendors themselves in a transient simulation program, but these models are not portable to other software, they may not scale up to large

grid studies, and they may not be robust under a variety of simulated conditions. Confidentiality agreements have also been a barrier to the use of custom models from hardware vendors. For all these reasons, it has not been possible to validate these models or use them with confidence in studies. The IEEE P1547.1 working group has proposed new tests for inverter-based DER, but these have not been adopted yet and they do not completely characterize the important responses of inverter-based DER.

One approach to closing this gap would be the following:

1. Develop new type tests to support new models.
2. Perform the tests on many specimens.
3. Develop new models that use parameters from the new tests.
4. Implement practical models in open-source software.
5. Link those models to utility-grade software.

When standardized, technology vendors would routinely provide the type test data, so that commercial software vendors could then implement models that accept type test data. As a result, a protection engineer should be able to determine, with the necessary confidence, whether a new relay scheme (e.g., Figure 4.12) will work or not on a specific feeder.

9.3 Long-Term Research Needs

Some other gaps were identified during this study that will require longer-term research programs, potentially longer than three years. A comprehensive roadmap should account for them. The gaps are the following:

- Cost-effective sensors are necessary for advanced relaying schemes, including
  - precision timing for traveling-wave relays
  - high-fidelity voltage and current sensors for traveling-wave relays, and high-frequency signal processing methods like incremental distance
  - voltage sensors for network protector vaults, which have limited space and may be submerged.
- New signal processing algorithms are needed for high-penetration DER, including
  - microgrids operating in different modes
  - fault and switching event identification for traveling wave and incremental distance relays.
- A streamlined on-ramp for promising new methods is needed to move from research to field evaluation and then deployment.

10.0 Next Steps

An early version of this report was presented at U.S. Department of Energy (DOE) headquarters on April 5, 2018, and elements of it were discussed with industry peer reviewers at a session in Oak Ridge, Tennessee, on July 18–19, 2018. A separate project with the DOE Solar Energy Technologies Office has been planned to evaluate promising new schemes for radial feeders. More work needs to be done on secondary network and microgrid protection; these issues should be among those addressed in a DOE roadmap for protection system research.

The rest of this section outlines general processes for evaluating new schemes, and for engaging with the utility industry on protection system research.

10.1 Test Plan for Lab and Field Evaluation

The evaluation process for each candidate protection scheme follows this framework:

1. Conceptual Design, which includes literature review, analytical modeling of the power system and protection functions, a peer review by industry protection experts, and outreach to potential demonstration utilities. This produces a candidate protection scheme and test site.
2. Model-Based Design, which includes transient or dynamic simulation of event scenarios with relay models in a transients program (e.g., ATP, EMTP-RV, PSCAD, MATLAB with SimPowerSystems) or a hardware-based simulator (e.g., OpalRT, RTDS). This produces the specifications and settings for relays and sensors.
3. Hardware Verification, which includes hardware-in-the-loop simulation of the protection scheme at the planned test site. It may be necessary to program utility-grade controllers or microcomputers to implement special algorithms. This step produces a detailed test plan for the demonstration.
4. Field Trial, which includes utility installation of the relays and sensors next to the existing protection. The new scheme will detect faults, but not trip. The trial should last at least six months, preferably longer. This step produces a report on verification, performance of the new scheme, and lessons learned.

10.2 Outreach Plan

There are several technical conferences that focus on protection. Outreach should include papers and panel sessions at these specialized conferences, which attract many more protection engineers than the IEEE Power & Energy Society (PES) General Meeting, Innovative Smart Grid Technologies (ISGT) conference, Transmission and Distribution (T&D) Conference, or DistribuTECH. The conferences of most interest include the following:

- Western Protective Relay Conference, Spokane, Washington. The next event is October 21–24, 2019. A conference paper based on results of this project was presented at the 2018 conference. (McDermott 2018).
- Georgia Tech Protective Relaying Conference, Atlanta, Georgia. The next event is April 29–May 1, 2020.
- Texas A&M Conference for Protective Relay Engineers, College Station, Texas. The next event is March 30–April 2, 2020.

- IEEE Power System Relaying Committee meets three times per year. This is a good networking opportunity. The next three meetings are
  - January 12–16, 2020, Jacksonville, Florida.
  - May 4–7, 2020, Nashville, Tennessee.
  - September 2020, dates and location to be determined.

11.0 References

Al-Nasseri H and MA Redfern. 2008. "Harmonics content based protection scheme for micro-grids dominated by solid state converters." In *12th International Middle-East Power System Conference*, pp. 50–56. Aswan, Egypt.

Al-Nasseri H, MA Redfern, and F Li. 2006. "A voltage based protection for micro-grids containing power electronic converters." In *IEEE Power Engineering Society General Meeting*, pp. 7. Montreal, Quebec, Canada.

Anderson K, M Coddington, K Burman, S Hayter, B Kroposki, and A Watson. 2009. "Interconnecting PV on New York City's Secondary Network Distribution System." City University of New York, NY. Available: https://www.nrel.gov/docs/fy10osti/46902.pdf.

Arritt RF and RC Dugan. 2008. "Distributed generation interconnection transformer and grounding selection." In *2008 IEEE Power and Energy Society General Meeting - Conversion and Delivery of Electrical Energy in the 21st Century*, pp. 1–7. Pittsburgh, Pennsylvania.

Arritt RF and RC Dugan. 2010. "The IEEE 8500-node test feeder." In *2010 IEEE/PES Transmission and Distribution Conference and Exposition: Latin America (T&D-LA)*, pp. 1–6. Sao Paulo, Brazil.

Arritt RF and RC Dugan. 2015. "Review of the impacts of distributed generation on distribution protection." In *2015 Rural Electric Power Conference (REPC)*, pp. 69–74. Asheville, NC. DOI: 10.1109/REPC.2015.12.

Baier M, WE Feero, and DR Smith. 2003. "Connection of a distributed resource to a 2-transformer spot network." In *2003 IEEE PES Transmission and Distribution Conference and Exposition*, Dallas, TX. DOI: 10.1109/TDC.2003.1335328.

Benitez M, J Xavier, K Smith, and D Minshall. 2017. "Directional element design for protecting circuits with capacitive fault and load currents." In *Annual Western Protective Relay Conference*, Spokane, WA.

Blumschein J, C Dzienis, and M Kereit. 2014. "Directional comparison based on high-speed-distance protection using delta quantities." Presented at the *Western Protective Relay Conference*, Spokane, WA.

Bokhari A, A Raza, M Diaz-Aguilo, F de Leon, D Czarkowski, RE Uosef, and D Wang. 2016 "Combined effect of CVR and DG penetration in the voltage profile of low-voltage secondary distribution networks." *IEEE Transactions on Power Delivery* 31(1):286–293.

Choudhary NK, SR Mohanty, and RK Singh. 2014. "A Review on Microgrid Protection." In *2014 International Electrical Engineering Congress* (iEECON), pp. 1–4, Pattaya, Thailand.

Conti S, L Raffa, and U Vagliasindi. 2009. "Innovative solutions for protection schemes in autonomous MV micro-grids." In *2009 International Conference on Clean Electrical Power*, pp. 647–654, 9–11 June 2009, Capri, Italy. DOI: 10.1109/ICCEP.2009.5211985.

Dewadasa JM, A Ghosh, and G Ledwich, 2008a. "Distance protection solution for a converter controlled microgrid." In *Fifteenth National Power Systems Conference (NPSC)*, IIT Bombay.

Dewadasa M, A Ghosh, and G Ledwich. 2008b. "Line protection in inverter supplied networks." In the *2008 Australasian Universities Power Engineering Conference*, pp. 1–6, Sydney, Australia.

Dewadasa M, A Ghosh, and G Ledwich. 2009. “An inverse time admittance relay for fault detection in distribution networks containing DGs.” In *TENCON 2009 - 2009 IEEE Region 10 Conference*, pp. 1–6, Singapore.

Dewadasa M, A Ghosh, and G Ledwich. 2011. “Protection of microgrids using differential relays.” In *Australasian Universities Power Engineering Conference (AUPEC)*, pp. 1–6, Brisbane, Queensland, Australia.

DSASC – Distribution System Analysis Subcommittee. 2019. “Test Feeder Working Group”. Available: http://sites.ieee.org/pes-testfeeders/resources. Accessed on: 2019/09/13.

Dusang LV and BK Johnson. 2008. “Evaluation of fault protection methods using ATP and MathCAD.” In *2008 IEEE Canada Electric Power Conference*, pp. 1–8, Vancouver, BC, Canada.

Glass J, AM Melin, MR Starke, and B Ollis. 2016. *Chattanooga Electric Power Board Case Study Distribution Automation*. ORNL/LTR--2015/444. Oak Ridge National Laboratory, Oak Ridge, TN. Available: https://www.osti.gov/scitech/biblio/1329733-chattanooga-electric-power-board-case-study-distribution-automation. Accessed on: 2017/12/19/19:59:58.

Guzmán A, B Kasztenny, Y Tong, and MV Mynam. 2018. “Accurate and economical traveling-wave fault locating without communications.” In the *71st Annual Conference for Protective Relay Engineers* (CPRE), pp. 1–18, College Station, TX.

Haron AR, A Mohamed, H Shareef, and H Zayandehroodi. 2012. “Analysis and Solutions of Overcurrent Protection Issues in a Microgrid.” In *2012 IEEE International Conference on Power and Energy (PECon)*, pp. 644–649, Kota Kinabalu, Malaysia.

Hartmann W. 2017. “Advanced feeder protection applications.” In *2017 Annual Pulp, Paper and Forest Industries Technical Conference (PPFIC)*, pp. 1–6, Tacoma, Washington.
DOI: 10.1109/PPIC.2017.8003863

Hatziargyriou N. 2014. “Microgrid Protection.” Chapter 4 in *Microgrids: Architectures and control*. First edition (March 3, 2014), Wiley-IEEE Press.

Horak J. 2006. “Directional overcurrent relaying (67) concepts.” In *IEEE 59th Annual Conference for Protective Relay Engineers*, College Station, TX.

IEC – International Electrotechnical Commission. 2019. Standard 61850, *Communication Networks and Systems in Substations*. Geneva, Switzerland. Available at https://www.iec.ch/smartgrid/standards/.

IEEE - The Institute of Electrical and Electronics Engineers. 2011. *IEEE Recommended Practice for Interconnecting Distributed Resources with Electric Power Systems Distribution Secondary Networks*, pp. 1–38, IEEE Std 1547.6-2011.

IEEE - The Institute of Electrical and Electronics Engineers. 2012. *IEEE Guide for Electric Power Distribution Reliability Indices*, pp. 1–43, IEEE Std 1366-2012 (Revision of IEEE Std 1366-2003).

IEEE - The Institute of Electrical and Electronics Engineers. 2013. *IEEE/IEC Measuring Relays and Protection Equipment – Part 24: Common Format for Transient Data Exchange (COMTRADE) for Power Systems*, pp. 1–73, IEEE Std C37.111-2013 (IEC 60255-24 Edition 2.0 2013-04).

IEEE - The Institute of Electrical and Electronics Engineers. 2016. *IEEE Recommended Practice for Excitation System Models for Power System Stability Studies*, pp. 1–207, IEEE Std 421.5-2016 (Revision of IEEE Std 421.5-2005).

IEEE - The Institute of Electrical and Electronics Engineers. 2018. *IEEE Standard for Interconnection and Interoperability of Distributed Energy Resources with Associated Electric Power Systems Interfaces*, pp. 1–138, IEEE Std 1547-2018 (Revision of IEEE Std 1547-2003).

Kar S and SR Samantaray. 2014. "Time-frequency transform-based differential scheme for microgrid protection." *Transmission Distribution IET Generation* 8(2):310–320.

Kersting WH. 2001. "Radial distribution test feeders." In *2001 IEEE Power Engineering Society Winter Meeting Conference Proceedings* (Cat. No.01CH37194), 2, 908–912, Columbus, OH.

Li X, A Dyśko, and GM Burt. 2014. "Traveling wave-based protection scheme for inverter-dominated microgrid using mathematical morphology." *IEEE Transactions on Smart Grid* 5(5):2211–2218.

Marti JR. 1982. "Accurate modelling of frequency-dependent transmission lines in electromagnetic transient simulations." *IEEE Transactions on Power Apparatus and Systems*, PAS-101(1):147–157.

McCarthy C and D Staszesky. 2008. "Advancing the state of looped distribution feeders." Presented at *DistribuTECH*, Tampa, FL. Available: http://www.sandc.com/globalassets/sac-electric/documents/sharepoint/documents---all-documents/technical-paper-766-t83.pdf.

McCarthy C, R O'Leary, and D Staszesky. 2008. "A new fuse-saving philosophy." Presented at *DistribuTECH*, Tampa, FL. Available: http://www.sandc.com/globalassets/sac-electric/documents/sharepoint/documents---all-documents/technical-paper-766-t84.pdf.

McDermott TE, T Smith, J Hambrick, A Barnes, R Fan, B Vyakaranam, P Thekkumparmathmana, and Z Li. 2018. "Protective Relaying for Distribution and Microgrids Evolving from Radial to Bi-Directional Power Flow." Presented at *Western Protective Relaying Conference*, Spokane, WA.

Memon AA and K Kauhaniemi. 2015. "A critical review of AC microgrid protection issues and available solutions." *Electric Power Systems Research*, 129(Supplement C):23–31. https://doi.org/10.1016/j.epsr.2015.07.006.

Mohammadi P and S Mehraeen. 2017. "Challenges of PV integration in low-voltage secondary networks." *IEEE Transactions on Power Delivery*, 32(1):525–535.

National Grid. 2018. *Supplement to Specifications for Electrical Installations: Requirements for Parallel Generation Connected to a National Grid Owned EPS*, version 4.0. Available: https://www9.nationalgridus.com/non_html/shared_constr_esb756.pdf.

Nikkhajoei H and RH Lasseter. 2006. "Microgrid fault protection based on symmetrical and differential current components." *Power System Engineering Research Center*.

OE – U.S. DOE Office of Electricity. 2016. *Advanced Metering Infrastructure and Customer Systems: Results from the Smart Grid Investment Grant Program.* Available: https://www.energy.gov/sites/prod/files/2016/12/f34/AMI%20Summary%20Report_09-26-16.pdf.

PG&E – Pacific Gas and Electric Company. 2018. Unit cost guide. Available: https://www.pge.com/pge_global/common/pdfs/for-our-business-partners/interconnection-renewables/Unit-Cost-Guide.pdf.

Passey R, T Spooner, I MacGill, M Watt, and K Syngellakis. 2011. "The potential impacts of grid-connected distributed generation and how to address them: A review of technical and non-technical factors." *Energy Policy*, 39(10):6280–6290.

Perera N and AD Rajapakse. 2006. "Agent-based protection scheme for distribution networks with distributed generators." In *2006 IEEE Power Engineering Society General Meeting*, pp. 6, Montreal, Quebec, Canada.

Saleh SA. 2014. "Signature-coordinated digital multirelay protection for microgrid systems." *IEEE Transactions on Power Electronics*, 29(9):4614–4623.

Samantaray SR, G Joos, and I Kamwa. 2012. "Differential energy based microgrid protection against fault conditions." In *2012 IEEE PES Innovative Smart Grid Technologies* (ISGT ASIA 2012), pp. 1–7, Tianjin, China.

Schneider K, P Phanivong, and JS Lacroix. 2014. "IEEE 342-node low voltage networked test system." In *2014 IEEE PES General Meeting | Conference & Exposition*, pp. 1–5, National Harbor, MD.

Schweitzer EO and B Kasztenny. 2017. Distance Protection: Why Have We Started with a Circle, Does it Matter, and What Else is Out There?" In *Western Protective Relay Conference*, Spokane, WA. Available at https://doi.org/10.1109/CPRE.2018.8349791.

Schweitzer EO, A Guzmán, MV Mynam, V Skendzic, B Kasztenny, and S Marx. 2014. "Locating faults by the traveling waves they launch." In the *67th Annual Conference for Protective Relay Engineers*, pp. 95–110, College Station, TX.

Schweitzer EO, D Finney, and MV Mynam. 2012. "Applying radio communication in distribution generation teleprotection schemes." In *2012 65th Annual Conference for Protective Relay Engineers*, pp. 310–320, College Station, TX.

Sharaf HM, HH Zeineldin, and E El-Saadany. 2018. "Protection coordination for microgrids with grid-connected and islanded capabilities using communication assisted dual setting directional overcurrent relays." *IEEE Transactions on Smart Grid*, 9(1):143–151.

Shi S, B Jiang, X Dong, and Z Bo. 2010. "Protection of microgrid." *10th IET International Conference on Developments in Power System Protection (DPSP 2010)*, pp. 1-4, Managing the Change, Manchester, UK.

Sortomme E, SS Venkata, and J Mitra. 2010. "Microgrid protection using communication-assisted digital relays." *IEEE Transactions on Power Delivery*, 25(4):2789–2796.

Starke M, B Ollis, J Glass, A Melin, G Liu, and I Sharma. 2017. *Analysis of Electric Power Board of Chattanooga Smart Grid Investment*. Oak Ridge National Laboratory, Oak Ridge, TN. Available: https://www.osti.gov/scitech/biblio/1376469-analysis-electric-power-board-chattanooga-smart-grid-investment, Accessed on: 2017/12/19/20:02:31.

Tecogen Inc. 2018. *Inverde: Tecogen, Inc. (tgen)*. Available: https://www.tecogen.com/chp/inverde.

Teodorescu R, M Liserre, and P Rodriguez. 2011. *Grid Converters for Photovoltaic and Wind Power Systems*. John Wiley & Sons, Hoboken, New Jersey.

Vasquez JC, JM Guerrero, M Savaghebi, J Eloy-Garcia, and R Teodorescu. 2013. "Modeling, analysis, and design of stationary-reference-frame droop-controlled parallel three-phase voltage source inverters." *IEEE Transactions on Industrial Electronics*, 60(4):1271–1280.

Voima S, K Kauhaniemi, and H Laaksonen. 2011. "Novel protection approach for MV microgrid." *International Conference and Exhibition on Electricity Distribution, CIRED 2011*, Frankfurt, Germany.

Wang W, J Kliber, and W Xu. 2009. "A scalable power-line-signaling-based scheme for islanding detection of distributed generators." *IEEE Transactions on Power Delivery*, 24(2):903–909.

Distribution

No. of
Copies

Name
Organization
Address
City, State and ZIP Code

Organization
Address
City, State and ZIP Code
Name
Name
Name
Name
Name (#)

Name
Organization
Address
City, State and ZIP Code

No. of
Copies

Foreign Distribution
Name
Organization
Address
Address line 2
COUNTRY

Local Distribution
Pacific Northwest National Laboratory
Name Mailstop
Name Mailstop
Name Mailstop
Name Mailstop
Name (PDF)

Pacific Northwest
NATIONAL LABORATORY

www.pnnl.gov

902 Battelle Boulevard
P.O. Box 999
Richland, WA 99352
1-888-375-PNNL (7665)

U.S. DEPARTMENT OF
ENERGY